BIOACTIVITY AND BIOCOMPATIBILITY OF GLASS IONOMER CEMENT ADDED WITH MONOCALCIUM SILICATE AT VARIOUS RATIOS

A THESIS

BY

WIROJ SANGSAWATPONG

Presented in Partial Fulfillment of the Requirements for the

Master of Science Degree in Endodontology

at Srinakharinwirot University

October 2013

BIOACTIVITY AND BIOCOMPATIBILITY OF GLASS IONOMER CEMENT ADDED WITH MONOCALCIUM SILICATE AT VARIOUS RATIOS

A THESIS

BY

WIROJ SANGSAWATPONG

Presented in Partial Fulfillment of the Requirements for the

Master of Science Degree in Endodontology

at Srinakharinwirot University

October 2013

BIOACTIVITY AND BIOCOMPATIBILITY OF GLASS IONOMER CEMENT ADDED WITH MONOCALCIUM SILICATE AT VARIOUS RATIOS

AN ABSTRACT

BY

WIROJ SANGSAWATPONG

Presented in Partial Fulfillment of the Requirements for the

Master of Science Degree in Endodontology

at Srinakharinwirot University

October 2013

Wiroj Sangsawatpong. (2013). *Bioactivity and biocompatibility of glass ionomer cement added with monocalcium silicate at various ratios*. Master thesis, M.S.(Endodontology). Bangkok: Graduate School, Srinakharinwirot University. Advisor Committee: Dr. Jaruma Sakdee , Asst. Prof. Dr. Punnama Siriphannon.

Recently, several studies attempted to improve biological property of glass ionomer cement (GIC) by adding some bioactive ceramics to glass ionomer cement but their results were unclear. Monocalcium silicate (CS) is one of new bioceramics material which can rapidly induce hydroxyapatite crystals on its surface. Therefore, adding CS to GIC could promote biological property of GIC. The purpose of this study was to compare bioactivity and biocompatibility of GIC added with CS in three different ratios to glass ionomer cement and MTA. Twenty discs of mixture of GIC with 10%, 30% and 50% w/w CS, GIC and MTA were fabricated. Fifteen discs were immersed in simulated body fluid (SBF) for 7, 14, and 28 days. The remaining discs were kept in room temperature. All of samples were analysed under SEM, XRD and XRF to investigate the crystallization and elemental composition of sample surfaces. A total of 0.02 g of each group was seeded in 1 mL of cell culture media. The solution over the mould was used to evaluate cell viability by MTT assay. The results showed that consistent crystals grow on the surface of 50%CS-GIC and MTA which presented Ca/P ratio close to 1.67, theoretical value of hydroxyapatite. In case of MTT assay, it revealed that the more ratio of CS inclusion was added, the more cell viability increased. In conclusion, the inclusion of 50%CS increased bioactivity and biocompatibility of GIC.

ความเข้ากันได้ทางชีวภาพและกิจกรรมทางชีวภาพของกลาสไอโอโนเมอร์ซีเมนต์ที่ผสมโมโนแคลเซียมซิลิเกตในอัตราส่วนต่างๆ

บทคัดย่อ

ของ

วิโรจน์ แสงสวัสดิ์พงศ์

เสนอต่อบัณฑิตวิทยาลัย มหาวิทยาลัยศรีนครินทรวิโรฒ เพื่อเป็นส่วนหนึ่งของการศึกษา
ตามหลักสูตรปริญญาวิทยาศาสตร์มหาบัณฑิต สาขาวิชาทันตกรรมคลินิก(วิทยาเอ็นโดดอนท์)

ตุลาคม 2556

วิโรจน์ แสงสวัสดิ์พงศ์. (2556). *กิจกรรมทางชีวภาพและความเข้ากันได้ทางชีวภาพของกลาสไอโอโนเมอร์ซีเมนต์ที่ผสมโมโนแคลเซียมซิลิเกตในอัตราส่วนต่างๆ*. ปริญญานิพนธ์, วท.ม.(วิทยาเอ็นโดดอนท์). กรุงเทพฯ: บัณฑิตวิทยาลัย มหาวิทยาลัยศรีนครินทรวิโรฒ. อาจารย์ที่ปรึกษาปริญญานิพนธ์: อาจารย์ ทันตแพทย์หญิง ดร. จารุมา ศักดิ์ดี, ผู้ช่วยศาสตราจารย์ ดร. ปุณณมา ศิริพันธ์โนน.

เมื่อไม่นานมานี้มีนักวิจัยพยายามที่จะปรับปรุงคุณสมบัติทางชีวภาพของกลาสไอโอโนเมอร์ซีเมนต์โดยเติมเซรามิกส์ชีวภาพบางชนิดเข้าไปในส่วนผสมซึ่งผลการทดลองยังไม่ได้ข้อสรุปที่แน่ชัด โมโนแคลเซียมซิลิเกตเป็นวัสดุเซรามิกส์ชีวภาพที่น่าสนใจเนื่องจากสามารถสร้างผลึกไฮดรอกซีอะพาไทต์ได้อย่างว่องไว ดังนั้นการเติมโมโนแคลเซียมซิลิเกตในกลาสไอโอโนเมอร์ซีเมนต์น่าจะปรับปรุงคุณสมบัติทางชีวภาพของกลาสไอโอโนเมอร์ซีเมนต์ให้ดีขึ้นได้ จุดมุ่งหมายของการศึกษานี้คือเปรียบเทียบกิจกรรมทางชีวภาพและความเข้ากันได้ทางชีวภาพของกลาสไอโอโนเมอร์ซีเมนต์ที่ผสมโมโนแคลเซียมซิลิเกตในอัตราส่วน 10%, 30% และ 50% โดยน้ำหนัก กับกลาสไอโอโนเมอร์ซีเมนต์และเอ็มทีเอ ชิ้นงานถูกเตรียมเป็นแผ่นกลมจำนวน 20 ชิ้นจาก 5 กลุ่ม ชิ้นงานจำนวน 15 ชิ้นถูกแช่ในสารละลายที่มีความเข้มข้นของอิออนใกล้เคียงกับของเหลวในร่างกายมนุษย์เป็นระยะเวลา 7 วัน, 14 วัน และ 28 วัน ชิ้นงานที่เหลือเก็บไว้ที่อุณหภูมิห้อง เมื่อครบกำหนดระยะเวลา ชิ้นงานแต่ละชิ้นจะถูกตรวจหาความเป็นผลึกและส่วนประกอบทางเคมีบนพื้นผิวด้วยกล้องอิเล็กตรอนแบบส่องกราด, เอ็กซ์เรย์ดิฟแฟรกชั่น และ เอ็กซ์เรย์ฟลูออเรสเซนต์ ในขณะที่เตรียมตัวอย่างปริมาณ 0.2 กรัมเพื่อนำไปแช่ในอาหารเลี้ยงเซลล์ปริมาณ 1 มิลลิลิตรก่อนนำอาหารเลี้ยงเซลล์นี้ไปเลี้ยงเซลล์ ตรวจสอบความเป็นพิษต่อเซลล์ด้วยการวัดแบบเอ็มทีที ผลการทดลองพบผลึกอะพาไทต์บนผิวหน้าของกลุ่มกลาสไอโอโนเมอร์ซีเมนต์ที่ผสม 50% โมโนแคลเซียมซิลิเกตโดยน้ำหนักและสัดส่วนระหว่างธาตุแคลเซียมต่อฟอสฟอรัสใกล้เคียงกับ 1.67 ซึ่งเป็นค่าของไฮดรอกซีอะพาไทต์ ในขณะที่การทดสอบด้วยการวัดเอ็มทีที พบว่าเมื่อสัดส่วนของโมโนแคลเซียมซิลิเกตเพิ่มขึ้น จำนวนเซลล์ที่มีชีวิตรอดมากขึ้น โดยสรุป การใส่โมโนแคลเซียมซิลิเกตในปริมาณ 50% โดยน้ำหนักสามารถปรับปรุงคุณสมบัติทางชีวภาพของกลาสไอโอโนเมอร์ซีเมนต์ที่ดีขึ้นได้

The thesis titled

"Bioactivity and biocompatibility of glass ionomer cement added with monocalcium silicate at various ratios"

By

Wiroj Sangsawatpong

Has been approved by the Graduate School as partial fulfillment of the requirements for the Master of Science degree in Endodontology of Srinakharinwirot University

…… Dean of Graduate School

(Assoc. Prof. Dr. Somchai Santiwattanakul)

…Month Date Year…

Thesis Committee

…… Major-advisor

(Lect. Dr. Jaruma Sakdee)

…… Co-advisror

(Asst. Prof. Dr. Punnama Siriphannon)

Oral Defense Committee

…… Chair

(Dr. Wallapat Santaweesuk)

…… Committee

(Asst. Prof. Dr. Vantana Sattabunnasuk)

…… Committee

(Dr. Jaruma Sakdee)

…… Committee

(Asst. Prof. Dr. Punnama Siriphannon)

This research was supported by the grant

from

Graduate school, Srinakharinwirot University

ACKNOWLEDGEMENTS

First of all, I would like to thank Asst. Prof. Suwit Wimonchit and Dr. Jaruma Sakdee, my advisors, for their invaluable advices, concern and encouragement. I also would like to express my sincere grateful to Asst. Prof. Dr. Punnama Siriphannon, my co-advisor. She gave me a lot of valuable advices and knowledge in this research project. Without them, this thesis would never be completed successfully.

I am also grateful to Ms. Ratchaporn Srichan, Head of Tissue Culture Section, Research Institute, Faculty of Dentistry, Mahidol University, for providing human PDL fibroblast cell and valuable cell-cultured technical support.

Heartfelt thanks go to Ms. Supaporn Mala, scientist of Tissue Culture Section, Research Institute, Faculty of Dentistry, Mahidol University and Ms. Yuwanda Iamphoajeen, graduate student in Chemical Department, Faculty of Science, King Mongkut's Institute of Technology Ladkrabang for their helping and support.

Finally, I am deeply grateful to my dear family for all love and support.

Wiroj Sangsawatpong

TABLE OF CONTENTS

TABLE OF CONTENTS (continued)

TABLE OF CONTENTS (continued)

LIST OF TABLES

LIST OF FIGURES

LIST OF FIGURES (continued)

Figure Page

LIST OF ABBREVIATIONS

BMP	Bone morphogenetic protein
BSP	Bone sialoprotein
CaSR	Calcium sensing receptor
COL	Collagen
CS	Monocalcium silicate
DMEM	Dulbecco modified Eagle medium
DPBS	Dulbecco's phosphate-buffered saline
ECM	Extracellular matrix
EDX	Energy-dispersive X-ray spectroscopy
GIC	Glass ionomer cement
HEMA	Hydroxyethylmethacrylate
IL	Interleukin
IRM	Intermediate restorative material
ISO	International standard organization
mRNA	Messenger ribonucleic acid
MTA	Mineral trioxide aggregate
MTT	3-(4,5-dimethylthiazol-2- yl)-2,5-diphenyltetrazolium bromide

LIST OF ABBREVIATIONS (continued)

OD	Optical density
PBS	Phosphate-buffered saline
PHBV	poly(3-hydroxybutyrate-co-3-hydroxyvalerate)
PMMA	Poly methyl methacrylate
PDL	Periodontal ligament
PIXE	Particle induced X-ray emission
SBF	Simulated body fluid
SEM	Scanning electron microscope
Super EBA	Super ethoxy-benzoic acid
TEOS	Tetraethyl orthosilicate
XRD	X-ray diffraction
XRF	X-ray fluorescence

CHAPTER 1

INTRODUCTION

Background of present study

Since 1990s, Mineral trioxide aggregate or MTA has gained wide acceptance in endodontic practice including perforation repair, retrofilling, pulpotomy and apexification.[1] MTA has been shown to have proper physical properties, superior biocompatibility and sealing ability.[2,3] However, the drawbacks of MTA are relatively expensive, have long setting time and exhibit difficult handling properties.[4] Consequently, the search for a new cement with reduced setting time and good handling properties while having comparable biocompatibility and mechanical properties as MTA is underway.

The main composition of MTA is tricalcium silicate and dicalcium silicate.[5] The monophasic of either tricalcium silicate or dicalcium silicate has excellent *in vitro* bioactivity and biocompatibility but it has still long setting time and low mechanical strength at the early stage like MTA.[6,7] The biphasic tricalcium silicate[8,9] and dicalcium silicate[10] exhibit improved mechanical properties and bioactivity, and also reduced setting time. While these both types of bioactive ceramic continue to be the object of research and interest as substituted materials of MTA, monocalcium silicate has not been widely studied in dentistry. In fact, monocalcium silicate is a highly bioactive glass that can form a hydroxyapatite surface layer on exposure to simulated body fluid[11-14] and also to human parotid saliva.[15]Nevertheless, monocalcium silicate is brittle in nature.[16]

Glass ionomer cement (GIC) was introduced to dental application more than 25 years ago and has been shown to be a useful adjunct for restorative dentistry due to excellent chemical diffusion-based adhesion to enamel and dentin[17], minimized microleakage, thermal

biocompatibility with tooth enamel and dentin[18] and fluoride release.[19] The main composition of GIC is calcium-alumino-silicate glass powder and an aqueous solution of an acrylic acid homo- or copolymer.[20] Each type of GICs has different formulations and properties so that suitable for different clinical applications. Ketac™ Molar, one of the conventional GICs, was proposed to be used in endodontic application including root canal perforation repair and root-end filling materials. Costa *et al*[21] found that Ketac™ Molar and Fuji IX™ GP were the least cytotoxic to odontoblast cell line compared to other GICs. However, Vajrabhaya *et al*[22] showed that Ketac™ Molar extracts diminished the amount of viable PDL cells more than that of white ProRoot® MTA. The biocompatibility of white ProRoot® MTA can be observed from hydroxyapatite formation on its surface[5,23], which is not found on that of GIC. Therefore, the simplest way to improve the biological properties of GIC is adding a new material that could improve bioactivity and biocompatibility to GIC.

Recently, several studies attempted to improve biological property of glass ionomer cement (GIC) by adding some bioactive ceramics to glass ionomer cement but their results were controversial. Some papers resulted that mixture had better biological properties[24,25] and mechanical properties.[26] But other papers showed that bioactive GIC was difficult to be bioactive.[27,28] Up to the present time, there is no report of the combination of GIC and monocalcium silicate. It can be assumed that the combination of GIC and monocalcium silicate may result in biologically improved mixture. Nevertheless, the optimal ratio of each composition is still unknown. The aims of the present study were to investigate the *in vitro* bioactivity [presence of apatite crystals on material's surface when immersed in simulate body fluid (SBF)] and biocompatibility of GIC containing 10%, 30% or 50% (w/w) monocalcium silicate.

Research question

Which ratio of monocalcium silicate (CS) when mixed with GIC results in the best bioactivity and biocompatibility?

Research objectives

1. To examine the presence of the apatite crystals on the external surface of GIC-CS mixtures (10%, 30%, 50% CS by weight) when immersed in SBF

2. To examine the biocompatibility of GIC-CS mixtures (10%, 30%, 50% CS by weight) to PDL fibroblast cell compare with white ProRoot® MTA

Hypothesis

1. **Null hypothesis (H_0)**: the formation of apatite crystals on the external surface of GIC-CS mixtures (10%, 30%, 50% CS by weight) is not different from that of white ProRoot® MTA when immersed in SBF.

Alternative hypothesis (H_A): the formation of apatite crystals on the external surface of GIC-CS mixtures (10%, 30%, 50% CS by weight) is different from that of white ProRoot® MTA when immersed in SBF.

2. **Null hypothesis (H_0)**: the percentage of PDL fibroblast cell vitality indirectly contacted with GI-CS mixtures (10%, 30%, 50% CS by weight) is not different from that of white ProRoot® MTA.

Alternative hypothesis (H_A): the percentage of PDL fibroblast cell vitality indirectly contacted with GI-CS mixtures (10%, 30%, 50% CS by weight) is different from that of white ProRoot® MTA.

Field of research

To study the bioactivity of GIC-CS mixture by presence of apatite crystal on its surface when immersed in SBF and to compare the biocompatibility of GIC-CS mixture and white ProRoot™ MTA in PDL fibroblast cell by MTT assay

Keywords

Mineral trioxide aggregate, Glass ionomer cement, Monocalcium silicate, Simulated body fluid, Periodontal ligament fibroblast cell, MTT assay

Research design

Laboratory experimental study

Limitations

This is an *in vitro* study which may not represent clinical situation.

Benefits

If these mixtures have the optimal biological properties equally or better than white ProRoot® MTA, they have been further developed and used as the substitute material of white ProRoot® MTA.

Chapter 2

Literature review

The development of dental materials in 19th century results in today numerous dental cements possessing beneficially clinical application such as glass ionomer cement (GIC) and mineral trioxide aggregate (MTA). At present, GIC is popular in the restorative dentistry, mostly used for cavity lining, bases and filling materials. MTA is world-wide acknowledged as multi-proposed endodontic use such as pulpotomy, apexification, root-end filling and root perforation repair. In fact, they are made up from different chemical reactions which make them have unique mechanical, physical and biological properties.

Mineral trioxide aggregate

Mineral trioxide aggregate (MTA), firstly was introduced by Dr.Torabinejad and his co-workers in 1993[29] and patented in 1995.[30] In 1998, Dentsply Tulsa Corporation (Oklahoma, USA) manufactured commercial ProRoot™ MTA, which is grey in color and composed of 75% type I Portland cement, 20% Bismuth oxide for radiopacity and 5% gypsum.[31] The type I Portland cement commonly contains 4 major components that are tricalcium silicate (Ca_3SiO_5), dicalcium silicate (Ca_2SiO_4)[4], tricalcium aluminate ($Ca_3Al_2O_6$), and tetracalcium aluminoferrite (Ca_4AlFeO_5).[32] In order to minimize tooth discoloration effect from grey ProRoot™ MTA, white ProRoot™ MTA was developed by elimination of ferrite phase from all components.[33, 34] Many authors attempted to precisely evaluate the chemical composition and crystalline structure of ProRoot™ MTA powder. The details of these published papers are shown in Table 1.

Table 1 The composition and crystalline phase of white and grey ProRoot® MTA powder

Authors	Comparative	Instruments	Results	
			WMTA powder	GMTA powder
Asgary *et al* 2005[35]	Quantitative	Electron probe microanalysis	44.23% CaO 21.20% SiO_2 16.13% Bi_2O_3	40.45% CaO 17.00% SiO_2 15.90% Bi_2O_3 4.26% Al_2O_3 3.10% MgO 4.39% FeO
Camilleri *et al* 2005[33]	Qualitative	EDX analysis	Ca, Si, Bi, O	Ca, Si, Bi, O, Al, Fe
		XRD analysis	Ca_3SiO_5, Bi_2O_3	Ca_3SiO_5, Ca_2SiO_4, Bi_2O_3
Song *et al* 2006[36]	Quantitative	XRD analysis	56.7% Bi_2O_3 34.1% $Ca_3(SiO_4)O$ 0.9% $Mg_3(PO)_4$ 0.3% $Cu_5Si_6O_{17}.7H_2O$ 3.7% unknown 0.9% $CaCO_3$ 1.6% $Ca_4P_2O_9$ 1.7% Ca_2SiO_4	58.8% Bi_2O_3 30.3% $Ca_3(SiO_4)O$ 2.3% $Mg_3(PO)_4$ 5.3% $CaCO_3$ 1.0% $Ca_4P_2O_9$ 2.9% $Ca_2MgO.2AlFeO.6SiO.2O_5$
		EDX analysis	Ca, Si, C, O, Mg, Al, S, Bi	Ca, Si, C, O, Fe, Mg, Al, S, Bi
Belio-Reyes *et al* 2009[37]	Quantitative	XRD analysis	19.8% Bi_2O_3 51.9% Ca_3SiO_5 23.2% Ca_2SiO_4 3.8% $Ca_3Al_2O_6$ 1.3% $CaSO_4$	N/A
		EDX analysis with PIXE	O, Al, Si, Bi, S, Ca Fe, Ni, Cu, and Sr	N/A

Although MTA is mainly composed of Portland cement, the raw materials used for ProRoot® MTA are specially purified more than that used for the usual Portland cement.[38] Moreover, the aluminate phase, which acts as flux during the manufacture of the Portland cement, was scarcely found in MTA. These indicate that ProRoot® MTA was very likely manufactured in a laboratory rather than in a rotary kiln.[39]

Tricalcium silicate is the most important phase that reacts very quickly with water and can form 7 polymorphic crystalline phases which depend on temperature, composition or impurities.[40] The polymorphic crystalline phase is important because it has an influence on cement strength.[41] Dicalcium silicate normally reacts slowly with water. As a consequence, tricalcium silicate contributes to strength mainly up to 28 days, whereas dicalcium silicate gives a further strength at later age.[32] The tricalcium aluminate resulting from the addition of alumina in the mixture introduced into the kiln helps reduce the burning temperatures required to make cement. The aluminate phase formed in the cement reacts quickly with water and can promote an undesirable shortening of the setting time. It can be controlled by adding an agent such as gypsum which delayed the setting time.[32]

MTA cement was set by hydration reaction. This reaction takes place in 2 stages. Firstly, the calcium silicate powder reacts to water and results in the formation of calcium silicate hydrate (C-S-H) gel, which liberates calcium hydroxide. The calcium hydroxide then gradually reacts with the minerals to form other hydrated compounds.[39] The tricalcium silicate and the dicalcium silicate reactions are as follows[39]:

$$2(3CaO{\cdot}SiO_2) + 6H_2O \rightarrow 3CaO{\cdot}2SiO_2{\cdot}3H_2O + 3Ca(OH)_2$$

$$2(2CaO{\cdot}SiO_2) + 4H_2O \rightarrow 3CaO{\cdot}2SiO_2{\cdot}3H_2O + Ca(OH)_2$$

The calcium hydroxide released during and after completion of hydration process is a key factor of bioactivity of MTA.[39] The bioactivity of some biomaterials attributed to their

ability to produce hydroxyapaptite in the presence of phosphate contained solutions like simulated body fluid(SBF)[5,23,42] and Dulbecco's phosphate-buffered saline(DPBS)[43,44] Sarkar *et al*[5] found that calcium ions released from MTA reacted with the phosphate group in synthetic tissue fluid and formed hydroxyapatite-like apatite crystals [$Ca_{10}(PO_4)_6(OH)_2$] on its surface from calcium-phosphate reaction. This result is consistent with the work of Bozeman and his co-worker.[23] They reported that grey MTA and white MTA could form hydroxyapatite-like crystals in phosphate buffered solution. Additionally, Tay *et al*[42] reported that MTA could form beta-typed carbonate apatite known as biologic apatite representing the mineral phase of hard tissue after immersing white ProRoot® MTA in phosphate-buffered saline (PBS) for 10 days.

The formation of apatite comes from a role of hydrated silica gel.[45] After hydration, Ca^{2+} ions are rapidly released and migrated into the solution. Silicates are attacked by OH^- ions and formed Si-OH silanol on hydrated silicate gel layer which presents as negative surface charges. The SiO^- negative groups induce bond to liberated calcium ions (Ca^{2+}), positive charge. Then, the sorption of phosphate (PO_4^{3-}) or monohydrogenphophate (HPO_4^{3-}) ions occur and subsequently the nucleation of apatite phase was formed.[45] The details are shown in Figure1.

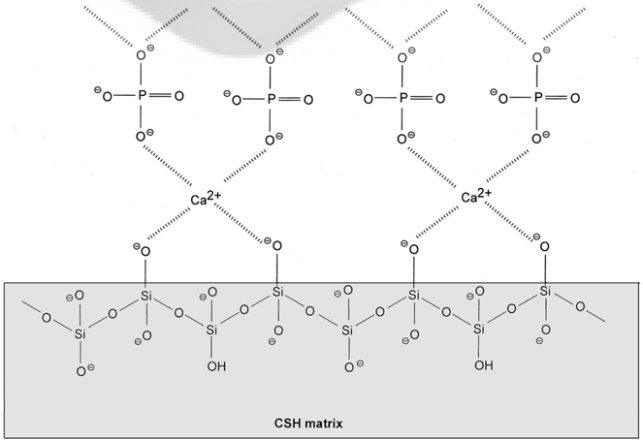

Figure 1 Ionic interactions between the CSH matrix and Ca^{2+} ions and the subsequent nucleation of an apatite phase[45]

From all of above, the physicochemical basis clarifies the three significant properties of MTA, namely, sealing ability, biocompatibility and dentinogenesis.[5] Tang *et al*[46] observed that MTA had the best leakage resistance to bacterial endotoxin amongst amalgam, IRM and super-EBA. Martin and his co-workers[47] also suggested that the apatite crystal deposition potentially obturated the space between MTA and root dentin and improved the seal of MTA apical plug with time. Additionally, Reyes-Carmona *et al*[48], who used scanning electron microscopic and x-ray diffraction to analyze the interface of MTA filled in dentin disk, also found that amorphous calcium phosphate precipitates with tag-like structures at the MTA cement-dentin interface. They concluded that the structures could be significant in minimizing leakage, influence the push-out bond strength and stimulate repair and dentinogenesis or cementogenesis.[49]

MTA has shown the superior *in vitro* biological properties. From the past, each study has used each method and each protocol to evaluate the biocompatibility of MTA. Almost all of them showed that MTA was the most biocompatible material amongst comparable materials. Moreover, some studies indicated that MTA was able to up-regulate the bone-forming gene, implied that MTA could promote the new hard tissue formation *in vivo*.

The direct contact study of Balto[50] who demonstrated that PDL fibroblast cell could tightly attached set-MTA surface but the cells shrank with many rough bleb in fresh-MTA. Al-rabeah *et al*[51] also demonstrated that human alveolar bone cells could attach and spread out on the surface of both grey and white ProRoot® MTA within 24 hours and could proliferate to form matrix-like layer within 7 days. These are in agreement with Paranjpe *et al*[52] who placed MTA in direct contact with human dental pulp cells. They found that the cells showed higher levels of osteocalcin and dentin sialoprotein which are the important odontoblastic gene for promoting the differentiation of the pulp cells into odontlblast-like cells. In addition, Thomson *et al*[53] demonstrated that OCCM-30 immortalized cementoblastic cell could attach and grow on MTA as well as the produce of alkaline

phosphatase (AP) and osteocalcin (OC) after 7 and 12 days. Abdullah *et al*[54] found that SaOS-2 osteosarcoma cells could not only adhere onto the surface of MTA without damage of cells but also up-regulate the levels of interleukin (IL)-1beta, IL-6, IL-18 and osteocalcin (OC).

Almost of indirect contact study clearly demonstrated that MTA was the best biocompatible as well. Keiser *et al*[55] who investigated the toxicity of both freshly and set mixed MTA extracts compared to amalgam and super-EBA found that MTA was the least toxic to PDL fibroblast cells amongst these materials in both freshly mixed and 24-hr set states. Moreover, Koulaouzidou *et al*[56] showed that survival rate of three different fibroblast cell lines against set ProRoot® MTA and glass ionomer cement (Fuji II™) were higher than IRM. Osorio *et al*[57] also confirmed that MTA is the least toxic root-end filling compared to amalgam, super-EBA, Ketac Silver and Gallium GF2.

Saidon *et al*[58] who indirectly co-cultured L929 mouse fibroblast cells with MTA and Portland cement extracts found that the number of cell co-cultured with fresh extracts of both materials was lower but the higher amount of the cells in set group. Bonson *et al*[59] showed that ProRoot® MTA could induce alkaline phosphatase activity in periodontal ligament fibroblast. Hakki *et al*[60] found that the concentration less than 0.02 mg/mL of MTA extracts could induce biomineralization and increased bone sialoprotein (BSP) and Collagen (COL)1 mRNA expression of OCCM-30 immortalized cementoblasts. Yasuda *et al*[61] showed that rat dental pulp cell cocultured with elunts of ProRoot® MTA was able to upregulate the level of bone morphogenetic protein (BMP)-2. This result is in agreement with Maeda *et al*[62] also reported that human periodontal ligament cell cocultured directly with ProRoot® MTA could upregulated BMP-2 expression and calcification. They believed that released calcium ions from MTA induced the BMP-2 and BMP-2 receptor through calcium sensing receptor (CaSR). Moreover, Takita *et al*[63] found that the pattern of released calcium ions from MTA is continuous and constant in early 14 days. They believed that released calcium ions could

play a greater role in the higher proliferation of human dental pulp cells. In addition, Tani-Ishii *et al*[64] demonstrated that white ProRoot® MTA could up-regulated the expression of type I collagen, BSP and OC in osteoblastic cell line after exposure 24 hours.

Nevertheless, Nakayama *et al*[65] who study toxicity of MTA to rat bone marrow cell by direct contact method found that MTA could suppress the differentiation of the cells. They also stated that pH value and the amount of released calcium ions did not influence cell growth.

A number of *in vivo* biocompatibility tests are in agreement with those *in vitro* cytotoxicity studies. Parirokh *et al*[66] who implanted white ProRoot® MTA, grey ProRoot® MTA and Calcium enriched cement (CEM) in albino rats' connective tissues found that all of specimens had less inflammation and presented the dystrophic calcifications in the connective tissue adjacent to these materials. Baek *et al,*[67] who retrofilled with MTA, amalgam and super-EBA in canines' teeth and determined the space between the filling material and the newly formed bone, found that the distance from MTA to the regenerated bone was similar to the normal average periodontal ligament thickness in dogs. Sousa *et al*[68] who implanted MTA, Zinc oxide eugenol and Z-100 light-cured composite resin as root-end filling material into mandible of guinea pigs found that MTA presented excellent biological qualities with bone growth in close contact with the material and no interposing connective tissue. Yalitrik *et al*[69] histopathologically examined the biocompatibility of MTA and high copper amalgam by implainting them into the dorsal connective tissues of rats for 7,15,30,60 and 90 days. They found favorable inflammatory response to MTA and amalgam at the 90-day observation period. They also found dystrophic calcification in connective tissue adjacent to MTA. This result is in agreement with Saidon *et al*[58] who found slight inflammatory response with new bone formation after implantation MTA and Portland cement into the guinea pigs' mandibles.

Another implicit property of MTA is dentinogenesis, which is also osteogenesis, cementogenesis and dentinal bridge as well. Zarrabi *et al,*[70] who used MTA as pulp-capped material in exposed human pulp, found that MTA could stimulate dentinal bridge formation. Economides *et al*[71] who used MTA and IRM as root-end filling material in non-inflamed dogs' teeth found the presence of moderate inflammation in early 3 weeks and then forming the new bone at the site of the resected apices after 2-5 weeks. Holland *et al*[72] who created the intentional lateral root perforations in dogs' teeth and repaired with MTA, also reported the deposition of cemental layer over that material in 180-day period. This result is in agreement with the histological study of Regan *et al*[73] who used MTA and Diaket as root-end filling in dogs' teeth. They also found the presence of complete cemental coverage over both the root end and MTA surface in 60-day period. Moreover, Apaydin *et al*[74] examined hard tissue healing adjacent to fresh or set MTA when used as root-end filling material in dogs. They found that cemental and osseous healing was uneventful in both groups.

Approved the advantageous properties by previous *in vitro* and *in vivo* studies, MTA has also shown a good clinical outcome especially root repair perforation materials. Main *et al*[75] found that their all 16 patients repaired with MTA showed the sign of healing after 1 year follow-up. Pace *et al*[76] also found that all ten cases repaired the furcal perforation with MTA showed clinical and radiographic healing after 5 years follow-up. De Chevigny and his co-worker,[77] who prospectively observed the success rate and associated predictors to failure from orthograde retreatment cases, also found that 4 of 16 cases repaired with MTA showed evident healing and turned the perforation which is the first predictor to failure(in their first phase) into the second.

Based on these findings, a great number of endodontists worldwide have adopted this material as the first choice in a range of applications from pulp capping to nonsurgical management of wide open apices. However, the drawbacks of MTA are difficult to control, unacceptably porous, dimensionally unstable, unacceptably soluble,[78] long setting time

and expensive.[5] Accordingly, several scientists have attempted to fabricate new material instead of MTA, including MTA Angelus (Angelus, Londrina, PR, Brazil) BioAggregate (Innovative Bioceramix, Vancouver, BC, Canada), Endosequence Root Repair Material (Brasseler, USA). However, the cost of these materials is not different from ProRoot® MTA.

Glass ionomer cement

Glass ionomer cement was firstly developed by Wilson and his colleagues in 1969 and introduced to dentistry field 2 years later for the aim to improve the esthetics of old-fashioned cements including zinc phosphate, zinc oxide eugenol and zinc polycarboxylate.[79] The commercially dental GIC was launched in 1972 and called ASPA (Alumino-Silicate-Poly-Acrylate) which literally illustrated the main chemicals of the glass and liquid.[18] The glass powder is aluminosilicate glass that containing calcium, fluoride, sodium and phosphate ions; as well, the liquid is polyacrylate acid and tartaric acid.[18] These weak acids dissolute the ionomer glasses to form solid cement. The acid-base reaction of GIC is categorized into 4 steps. The details are shown in Figure 2. Firstly, the protons (H^+) released from the acids attacking the glass network which result in the release of metallic ions, mainly Al^{3+}, Ca^{2+}or Sr^{2+}. Secondly, the cations migrated into the liquid phase. Thirdly, the interaction occurred while the cations and polyacid subsequently formed salt bridges between the polyacid chains and the formation of silica hydrogel. And GIC was finally hardening.[79] During the setting reaction, the liberated calcium ions faster reacted with the acid and cross-linked with the polyacrylic acid as calcium bridge to form calcium polycarboxylate gel. Then, the aluminum ions reacted with preformed matrix to form a water-insoluble Ca-Al-Carboxylate gel.[80] The acids only attacked the external surface of glass powder, whereas the glass core remained intact and acted as a reinforcing filler in the cement matrix.[80] The details of the chemical reaction of conventional GIC are shown in Figure 2.

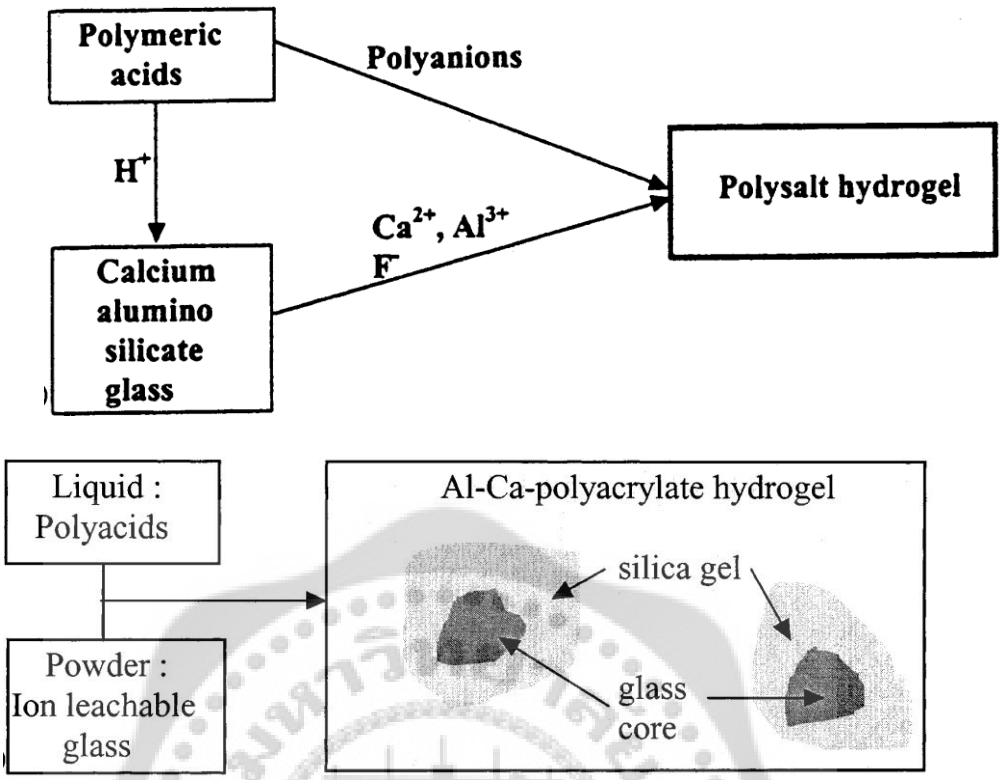

Figure 2 Chemical reaction process of glass ionomer cement[80]

The conventional GIC has many attractive properties including chemical bond to tooth structure, minimized microleakage, and thermal compatibility with tooth due to low thermal expansion coefficient.[18] However, because of its disadvantages including low mechanical strength, high water-sensitivity and long setting time,[81] it had been limitedly used in restorative field. Therefore, to overcome these inferior properties, the former conventional GIC had been developed in many variations of powder component and polycarbonic acid. From this result, today, GIC is well-suited for the wide range of clinical indications. The developed GIC is mainly categorized into 3 groups: reinforced conventional GIC, highly viscous conventional GIC and resin modified GIC.

Reinforced conventional GIC

One idea to increase cement strength and toughness is to incorporate metallic particles into the GIC matrix. By this concept, the so called “Cermets” [ceramic + cement] is derived. The Cermet powder is a mixture of conventional AgSn amalgam and the GIC glass particles and the liquid is polycarboxylic acid.[80] Zimehl *et al*[80] found that Cermet cement has an increased flexural strength and abrasion resistance compared to traditional GIC because the metallic particles might function as stress absorbers by reducing the friction coefficient and thereby being able to absorb the peak stresses. On the other hand, a few previous literatures demonstrated that physical properties were lower. Kilpatrick *et al*[82] showed that its durability as posterior restorative was poorer than conventional GIC. Sarkar *et al*[83] demonstrated that the metal-matrix interfacial bonding of Cermet was lacking. Williams *et al*[84] found that fluoride releasing from Cermet was lower than that of conventional GIC. The examples of commercially available reinforced conventional GIC are Ketac™ Silver (3M ESPE), Miracle Mix® (GC Chemical), Fuji II and Lumi-Alloy (GC Chemical).

Resin modified glass ionomer cement (RMGIC)

In 1980s, resin modified glass ionomer cement (RMGIC) was developed in order to overcome two main problems of conventional GICs: moisture sensitivity and the lack of command cure. RMGIC was developed by adding hydrophilic resin monomer (2-hydroxyethylmethacrylate, 2-HEMA) into the liquid part.[85] So, RMGIC has dual-curing mechanism which combined between acid-base reaction and the radical induced polymerization.[80] The introduction of light-cured systems of GIC exhibits extended working time, reduced the problems of moisture sensitivity, increased early mechanical strength, easy to handle and better esthetics.[79] Nevertheless, to compare with resin composite, the mechanical strength of RMGIC is still lower. This is because of hydrophilic functional groups within the structure of HEMA. It could take up large amount of water like ‘hydrogel’ and lead

to greater plasticity and reduction in strength.[80] Moreover, RMGIC has not significantly reduced the susceptibility of dehydration problems. So the maintenance of water balance in the modified cements is still of importance.[79] The examples of RMGIC are Vitrebond™ (3M ESPE), Vitremer™ (3M ESPE), Fuji II™ LC (GC), Geristore™ (Den-Mat Corporation).

Highly viscous conventional GIC

Highly viscous GIC was generally used because of rapid setting time, reduced moisture sensitivity in early stage of setting and minimal solubility in oral fluid.[20] The superior physical properties of highly viscous GIC come from development to optimizing the concentration and molecular weight of polyacid as well as the particle size distribution of the glass, which brings about high cross-linkage in the GIC matrix.[85] The examples of this GIC group are Ketac™ Molar (3M ESPE) and Fuji iX™ (GC)

Ketac™ Molar

Ketac™ Molar was manufactured by 3M ESPE manufacturing company in Seefeld, Germany. It was developed for the filling in proximal area and for atraumatic restorative treatment (excavated carious tooth structure and filled with GIC for reducing further chances of caries). Besides, it well suited for lining under composite fillings, core build up under crown, filling in primary tooth and Class I restoration in non-occluded region.[86]

Stamboulis *et al*[87] found that the crystalline powder is CaF_2, LaF_3, Al-F-Ca(*n*) by tracing with magic angle nuclear magnetic resonance (MAS-NMR). This is in agreement with the product literature[86] reported that the glass powder is aluminium-calcium-lanthanum-fluorosilicate glass powder. Moreover, the glass powder is modified for increasing the physical and mechanical properties by

1.) Adding dried-form polyacrylic to increase the mechanical properties without a remarkable change in its initial viscosity

2.) Minimizing the particle size of Ketac™ Molar powder (average 2 μm) for higher cross-linkage in Ketac™ Molar which leads to increase surface hardness and decrease water solubility

Ketac™ Molar has 2 packaging versions: hand mixed and automatically mixed capsule systems (APLICAP). Only the capsule systems contains 5% spray dried polycarbonate acid which is a copolymer from acrylic and maleic acid. The hand mixed version did not add. The manufacturer recommended the powder-liquid ratios (by weight) is 3:1 for hand mixed version and 3.4:1 for the APICAP which is already prepared in the capsule.[86] The details are shown in Table 2.

Table 2 Percentage of polyacid of Ketac™ Molar

Product	Powder/liquid ratio	Acid in powder	Acid in liquid
Ketac™ Molar Applicap	3.4:1	25%	75%
Ketac™ Molar Hand mixed version	3.0:1	0%	100%

Peez and Frank[88] found that Ketac™ Molar Easymix had the highest compressive strength and flexural strength value compared with the other viscous conventional GIC (Fuji IX™, Vitro Molar®, Vidrion R and Ionofil® Molar) with remarkably low solubility and acid erosion. Xie *et al*,[81] who studied the mechanical properties of various highly viscous conventional GIC and resin-modified GIC, found that Ketac™ Molar had the highest compressive strength within conventional GIC group.

Biological properties of glass ionomer cement

The details of chemical composition are varied in each GIC brand, so they have differences in biological effect to cells and tissues. However, previous paper demonstrated clearly that conventional GIC is more biocompatible than RMGIC. Costa *et al*,[21] who compared toxicity of five commercial GIC to odontoblastic cell line, found that Ketac™ Molar and Fuji IX™ GP were the least cytotoxic but Vitrebond™, Vitremer™ and Fuji II™ LC significantly lowered cell metabolism and caused remarkable cell death. Sengun *et al*[89] showed that immortalized odontoblast cell line slightly increased the survival rate after direct contact with Ketac™ Molar. Leyhausen *et al*,[90] who investigated the cytotoxicity of RMGIC (Ionoseal®, VOCO; Vitrebond™, 3M ESPE; Compoglass®, GC) and conventional GIC (Ketac™ Fil Application, 3M ESPE) to human gingival fibroblast and 3T3 mouse fibroblasts, reported that the extracts from Ketac™ Fil Application, Ionoseal® and Compoglass® slightly to moderately inhibited the proliferation of these cells whereas that from Vitrebond™ severely reduced the cell proliferation. This is similar to the result of Oliva *et al*[91] who investigated osteoblast viability co-cultured with four commercial GICs and reported that Vitremer™ was the most cytotoxic compared to Ketac™ Fil Aplicap, Ionocem Ionocap 1.0, GC Fuji II™ and GC Fuji II™ LC. They clarified that 2-hydroxyethylmethacrylate (HEMA) and an unidentified acidic species leached from the liquid part made Vitremer™ was the highest cytotoxic. Geurtsen *et al*[92] found that organic component substances releasing from Fuji II LC and Vitrebond caused cytotoxic effects. This cytotoxic effect came from chlorine benzene, iondine benzene and bromide benzene which were decomposition products of the initiator dephenyliodoniumchloride.

Compared to other dental cements, GIC usually showed more biocompatible than the others. Chong *et al*,[93] who histopathologically evaluated periradicular tissue response to Vitrebond™ (3M ESPE), reinforced zinc oxide eugenol cement (Kalzinol) and amalgam, found that Vitrebond™ caused the least severity of inflammation. However, after

introduction of MTA into dentistry field, all of studies claimed that MTA's biological properties were superior to GICs'. Vajrabhaya *et al*[22] reported that Ketac™ Molar inhibited the growth of PDL cell and its cytotoxicity was greater than ProRoot® MTA. Abdullah *et al*[54] also reported that SaOs-2 osteosarcoma cell was round-shaped and unable to adhere to GIC's surface but there was an increase in cell number adhering to MTA's surface in difference with MTA group. The key factor for MTA biocompatibility, bioactivity as well as good sealing ability comes from the formation of hydroxyapatite-like crystals on MTA-tissue or MTA-dentin interface.[5,23] Although GIC has been considered to be biocompatible material, it has not shown bioactive property. Therefore, some researchers have attempted to add some bioactive materials to GICs. Yli-Urpo *et al*,[24] who investigated *in vitro* bioactivity of the conventional GIC and light-cured GIC containing 10% and 30% bioactive glass, found that light cured GIC with 30%wt of BAG showed highest bioactivity. Loof *et al*[25] also found that presence of hydroxyapatite on hybrid material of calcium aluminate mixed with glass ionomer cement liquid after immersed in phosphate solutions for 7days. However, Kamitakahara *et al*[27] also evaluated the possibility of obtaining bioactive glass ionomer cement by analyzing apatite formation on the bioactive glass when immersed in SBF in the presence and absence of polyacrylic acid. They found that 0.1 ppm of polyacrylic acid inhibited the apatite formation, and concluded that it might be difficult to obtain the bioactive glass ionomer cement. These results indicated that polyacrylic acid suppressed the apatite forming ability of bioactive glass. Matsuya *et al*[28] also demonstrated that polyacrylic acid retarded hydroxyapatite formation.

Bioactive materials

There are two terms described the properties of the biomaterials, that are bioinert and bioactive. Bioinert materials have neither a positive nor a negative effect on bone growth, while the bioactive have the induction of specific biological activity such as a surface property that provides the bond between a material and living tissue without fibrous encapsulation.[94] Silicate glasses, glass-ceramics and hydroxyapatite are well known examples of bioactive materials. The main element composition of these bioactive glasses and glasses-ceramics contained calcium and phosphate which is related to the main components of hard tissue (bone dentin and cementum).[95] Many previous studies showed that hydroxyapatite [$Ca_{10}(PO_4)OH_2$] and related CaPs support the adhesion, differentiation and proliferation of osteogenesis related cells (e.g. osteoblasts, mesenchymal stem cells).[96,97] This is obviously because of chemical composition. The calcium is known to affect osteoblastic cells. Previous studies showed that the low and medium (2-8 mmol) calcium concentrations are suitable for osteoblast proliferation, differentiation and extracellular matrix mineralization, respectively, but higher Ca concentration (>10 mmol) are cytotoxic.[98] Moreover, the bioactivity of these materials also depends on surface roughness, porosity, topography, grain size and crystallinity.[95]

Silicate-based cement

Another family of bioceramics is silicate-based cement introduced by Hench *et al* in 1972, now called 45S5 Bioglass® (wt%: $45SiO_2$-$25CaO$-$25Na_2O$-$6P_2O_5$).[95] Up to now, many published papers have been reported a good biological properties as biomedical applications. Xynos *et al*[99] found that ionic products of 45S5 Bioglass® increased osteoblast number to 150%. Tsigkou *et al*[100] also demonstrated that the glass extracts could promote osteoblast differentiation and extracellular matrix (ECM) deposition and mineralization. The key factor might be from released ions including calcium and silicate. Gough *et al*[101]

reported that lower concentration of Si facilitated mineralization and nodule formation of osteoblast cells, whereas the higher Si concentration led to cell apoptosis. Valerio *et al*[102] suggested that higher osteoblastic proliferation and collagen secretion after treatment with BG60S bioglass dissolution products were related to Si contact, since despite higher Ca concentration, unchanged osteoblast activity was observed in presence of biological calcium phosphate (no Si release). This result is similar to that of Kim *et al*[103] who found that Si supplementation reduced the bone resorption rate in Ca-deficient rats.

Monocalcium silicate

Like other silicate-based cements, monocalcium silicate ($CaSiO_3$) has been considered osseous repair or replacement. Monocalcium silicate ($CaSiO_3$), or Wallastonite, can bind to living bone through a hydroxyapatite layer when in contact with physiological fluid such as synthetic simulated body fluid (SBF),[11-14] and human parotid saliva.[15] Natural monocalcium silicate formed by the interaction of lime-stone with silica in hot magma.[104] In the present time, scientists can synthesize the monocalcium silicate in the laboratory called "pseudo-wollastonite". The synthesis by "sol-gel" technique produced the powder with an apatite-formation capacity when placed in simulated body fluid.[105] Siriphannon *et al*[13] found that monocalcium silicate powder synthesized by "co-precipitation" technique was rapidly observed the new hydroxyapatite layer and completely covered the surfaces within 5 days on exposure to simulated tissue fluid. This formation rate is faster than those of other bioactive glasses.[11]

Use of monophasic monocalcium silicate has been widely researched. Lin et al[106,107] demonstrated that sintered macroporous calcium silicate ceramic had optimum mechanical strength and could promote the bone marrow stem cell proliferation. Ni *et al*[108] also reported that osteoblastic cells were able to adhere and grew on porous monocalcium silicate scaffold as well as alkaline phosphatase activity of cells was improved. Moreover, De

Aza *et al*[109] who implanted the monocalcium silicate into rats' tibias and found that osteoblastic cell colonized on the implant's surface.

Monocalcium silicate-based composites

Due to the brittle nature of monocalcium silicate.[16] Recently, the combination of mono-calcium silicate and other polymers or composite materials for hard tissue repair has been interesting. Li and Chang[110,111] fabricated the composite scaffold of monocalcium silicate and poly(3-hydroxybutyrate-co-3-hydroxyvalerate) (PHBV) thermoplastic polyester and they found that composite materials showed good bioactivity, hydrophilicity, mechanical strength, and had pH buffering effect to degradation product of PHBV. Pattanayak[112] demonstrated that the composition of monocalcium silicate and poly methyl methacrylate (PMMA) as bone substitute rapidly produced apatite crystals on composite surface. Besides, the composition of monocalcium silicate glass and methyl methacrylate prepared by Monvisade *et al*[113] showed that compressive strength was in range of cortical bone.

CHAPTER 3

MATERIALS AND METHODS

Preparation of beta-monocalcium silicate

Beta-monocalcium silicate was prepared by co-precipitation method as described by Siriphannon *et al* in 2002.[13] Briefly, $Ca(NO_3)_2.4H_2O$ and $Si(OC_2H_5)_4$ (TEOS) were dissolved in 500 ml of ethanol under continuous stirring. The precipitate was obtained by the addition of 0.33 mol/l NaOH solutions into the above solution. The precipitated gel was filtered, washed twice with distilled water, dried in an oven at100°C overnight, and calcined at 500°C for 2 hours. The calcined powder was fired at 900°C for 2 hours to obtain beta-monocalcium silicate, low temperature crystalline phase. The resultant powder was ground and sieved through 230-mesh sieve before further use.

Preparation of the test materials

Ketac™ Molar (3M-ESPE Dental, Seefeld, Germany) was chosen as the baseline reference and white ProRoot® MTA (Densply Tulsa, OK, USA) was served as control. Beta-monocalcium silicate powder was added to Ketac™ Molar powder at three different weight ratios that are 10%, 30% and 50%. The mixed powder was then wetted from Ketac™ Molar liquid; the powder/liquid ratio was 3:1for Ketac™ Molar powder and 2.5:1 for $CaSiO_3$ powder. Ketac™ Molar and white ProRoot® MTA were prepared according to manufacturers' directions. The details are shown in Table 3.

Table 3 Preparation of all material groups

Groups	Powders	powders : liquid (w/w)
GIC	GIC (Ketac™ Molar)	3:1
10CS-GI	10% $CaSiO_3$ 90% GIC	2.94:1
30CS-GI	30% $CaSiO_3$ 70% GIC	2.83:1
50CS-GI	50% $CaSiO_3$ 50% GIC	2.73:1
MTA	White ProRoot® MTA	3.3:1

In vitro bioactivity test

Preparation of simulated body fluid solution

Simulated body fluid (SBF) is a synthetically physiological solution which has ion concentrations similar to those in human blood plasma. In this study, The SBF preparation followed the procedure described by Kokubo in 1990.[114] The details of ion concentrations of SBF solution and blood plasma are shown in Table 4

Table 4 Ion concentrations of simulated body fluid

	Ion concentration (mM)						
	Na^+	K^+	Mg^{2+}	Ca^{2+}	Cl^-	HCO^-	HPO^-
Simulated tissue fluid	142.0	5.0	1.5	2.5	148.8	4.2	1.0
Blood plasma	142.0	5.0	1.5	2.5	103.0	27.0	1.0

In Vitro immersion in simulated body fluid

Each group was mixed as previously described on a glass slab with stainless steel spatula. The fresh cement was rapidly placed in split stainless steel mold to obtained discs (10 mm in diameter and 3 mm in height). The excess cement was removed by cement spatula. The partially set cement was removed from the mold and kept in 37°C, 100% relative humidity chamber for 24 hours to allow completed set.

After incubation, each disc from all groups was immersed in 100 mL of SBF solution containing in screw-capped plastic bottle at 37°C for 7, 14 and 28 days. After the pre-selected soaking time, the discs were gently rinsed with deionized water to remove SBF solution followed by drying at room temperature. An un-immersed disc from all groups was served as baseline data.

The bioactivity of the specimens was assessed the evidence based on the hydroxyapatite formation on the disc surface after immersion in SBF solution. Scanning electron microscope (SEM, JEOL JSM-6510LV, Tokyo, Japan) was used to determine crystalline morphology. X-ray diffraction analysis (XRD, Bruker AG, D8 Advance, USA) was used to identify and characterize crystalline phase. Moreover, the chemical composition especially calcium and phosphate of unsoaked and 28-day-soaked specimens were carried out by X-ray fluorescence spectrometry (XRF, EDXRF EAGLE II, NJ, USA).

Biocompatibility test

PDL fibroblast cell culture

The protocol of the study was approved by the Ethics Committee of Faculty of Dentistry, Srinakharinwirot University. Human periodontal ligament (PDL) fibroblast cells were donated from Ms. Ratchaporn Srichan (Head of Tissue Culture section, Research Institute, Faculty of dentistry, Mahidol University, Thailand). Three cryogenic vials storing

frozen human PDL fibroblast cells from 3 unidentified persons were thawed and transferred into tissue culture flasks (Nunc, Thermo Scientific, Denmark) containing culture medium. The culture medium was Dulbecco's modified Eagle medium (DMEM) (Gibco, Grand Island, NY) supplemented with 10% fetal bovine serum (Hyclone, Thermo Scientific, Logan, UT, USA) and 1% antibiotic/antimycotic solution (10,000 U penicillin, 10 µg streptomycin, 25 µg amphotericin B per mL). Cells were maintained at 37°C, 5% CO_2 and 100% humidity in an incubator. After a confluent monolayer was obtained, cells were trypsinized and subcultured. The PDL fibroblast cells from 4^{th}-7^{th} passage were used in this study.

Preparation of material extracts

After mixing as previously described under aseptic condition, a total of 0.2 g of fresh cements was placed into a well of 24-well tissue culture plates. The specimens from three test groups and GIC group were kept in an incubator at 37 °C and 100% relative humidity for 30 minutes, whereas MTA specimens were kept for 4 hours in the same condition. After incubating, the specimens were exposed to ultraviolet light for 30 minutes to sterile. One milliliter of complete DMEM was poured into each well containing each specimen and incubated in the incubator for 72 hours. After incubating, extract from each well was transferred into a centrifugal vial for centrifugation for 5 minutes. The supernatant was collected and serially diluted 1:1 with DMEM to achieve a total of 4 concentrations. A series of extracts of different concentrations were made to observe a possible dose-response relationship.

Cell viability test (MTT assay)

Human PDL fibroblast cells were seeded into 96-well plates at 20,000 cells/well and incubated for 24 hours to allow attachment. Then, 100 µL of extract was placed into the tissue culture well. Cells with 100 µL culture medium served as a control. After an incubation, cell viability was evaluated by 3-(4,5-dimethylthiazol-2- yl)-2,5-diphenyltetrazolium bromide (MTT) assay. Briefly, the extract from each well was discarded,

washed once with 100 µL of phosphate-buffered saline (PBS), added 50 µl of MTT solution (1 mg/ml in PBS) and incubated for 2 hours. Subsequently, the MTT solution from each well was discarded and added 100 µl of isopropanol to each well. The plates were then shaken 30 minutes until the crystals had dissolved. Reduced MTT was then measured spectrophotometrically at 570 nm in a microtiter plate reader (BIO-TEK Instrument Inc, Winooski, VT). The optical density (OD) values of test wells and control wells were calculated by using the following formula:

$$\% \text{ cell viability} = \frac{\text{OD value of test well}}{\text{OD value of control well}} \times 100$$

The results were expressed as means ± standard deviations (SD). Experimental data were analysed by one-way ANOVA at significant level of $p < 0.05$. Post hoc tests were done with Scheffé's test. For this study, the experiment was repeated six replicates for each cell line.

Cell morphology

The images of PDL fibroblast cells treated with four concentrations of five materials' extracts were examined by using phase contrast microscope (Nikon TS-100-F, Nikon, Tokyo, Japan).

CHAPTER 4

RESULTS

In vitro bioactivity test

XRD analysis

The synthesized monocalcium silicate powder used in this study was characterized by X-ray diffraction (XRD) analysis which then showed the crystalline peaks corresponding to beta-monocalcium silicate (2 theta = 25.3, 26.9, 33.6, 34.1, 36.1 and 39.1°, and cristobalite (2 theta = 22°) (Fig.3). On the other hand, the as-received Ketac™ Molar used in this study was composed of 4 main peaks at 2 theta = 27.3, 31.6, 45.2 and 53.5° (Fig.4).

No noticeable change in peak pattern could be revealed after soaking GI specimens in the SBF solution for various times, still having the 4 main peaks of Ketac™ Molar powder (Fig.5). Contrarily, MTA specimens which soaked in the SBF solution for various times were different from the before soaking specimen. The XRD pattern of soaked specimens showed the crystalline peaks corresponding to hydroxyapatite, at 2 theta = 25.9, 31.8, 32.2, 32.9, 39.6, 46.5, 49.4, 50.5, and 51.2° (Fig.6).

Before soaking, specimens from the test groups i.e.10%CS-GI, 30%CS-GI and 50%CS-GI were observed the combined peak patterns of Ketac™ Molar, beta-monocalcium silicate and cristobalite. The intensity and quantity of the peaks depended on the GI/CS ratios. After soaking, the XRD patterns were mainly composed of Ketac™ Molar and cristobalite, whereas peaks of beta-monocalcium silicate decreased. No hydroxyapatite phase was found (Fig 7-9).

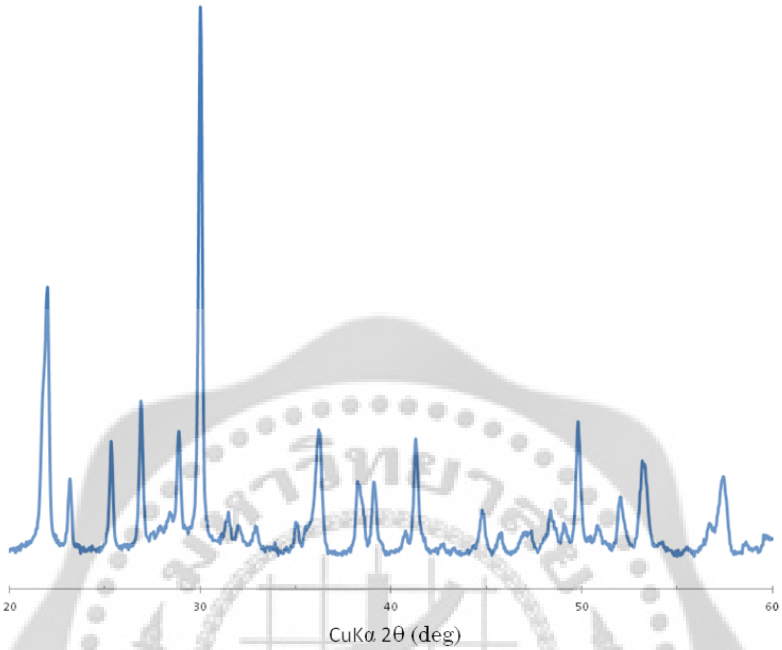

Figure 3 XRD patterns of synthesized beta- monocalcium silicate powder

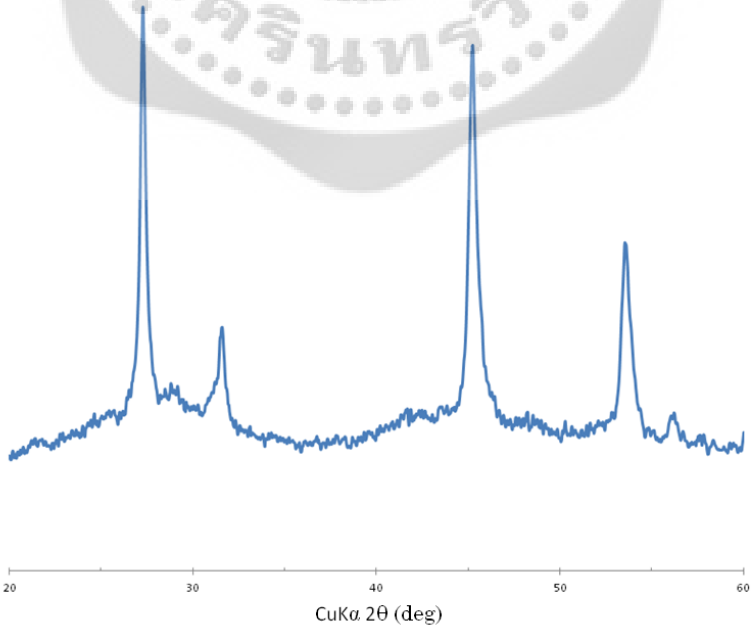

Figure 4 XRD patterns of Ketac™ Molar powder

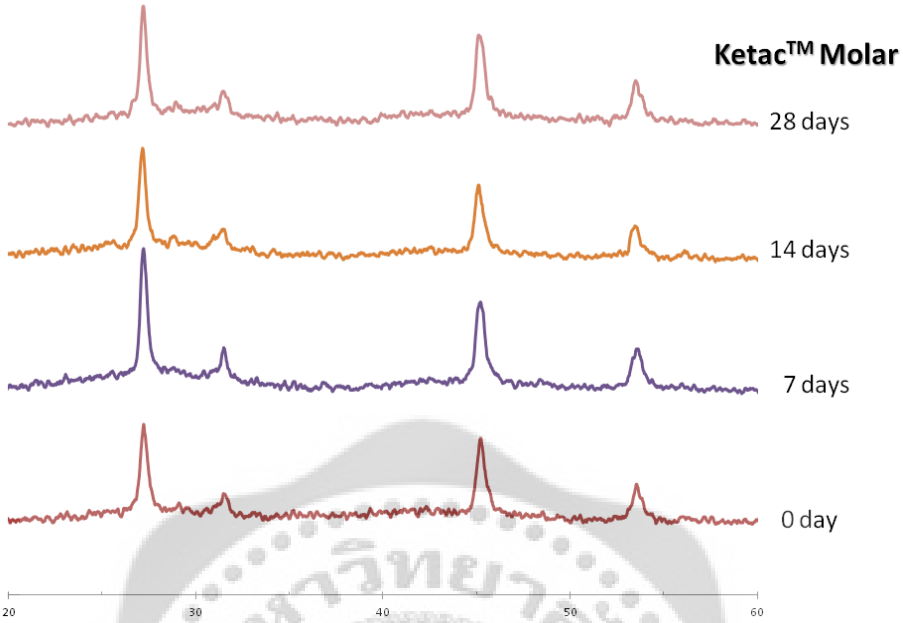

Figure 5 XRD patterns of GIC specimens before and after soaking in the SBF for various times

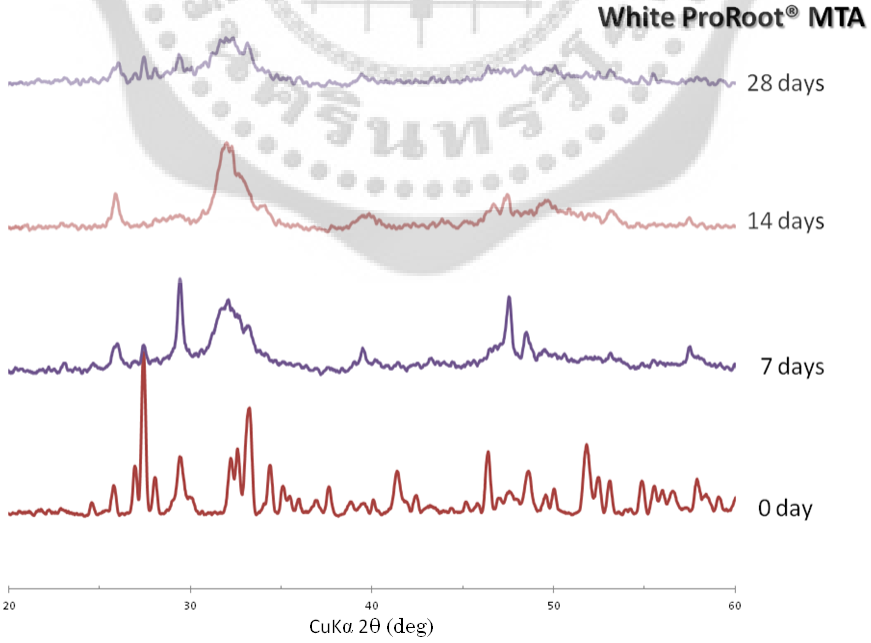

Figure 6 XRD patterns of MTA specimens before and after soaking in the SBF for various times

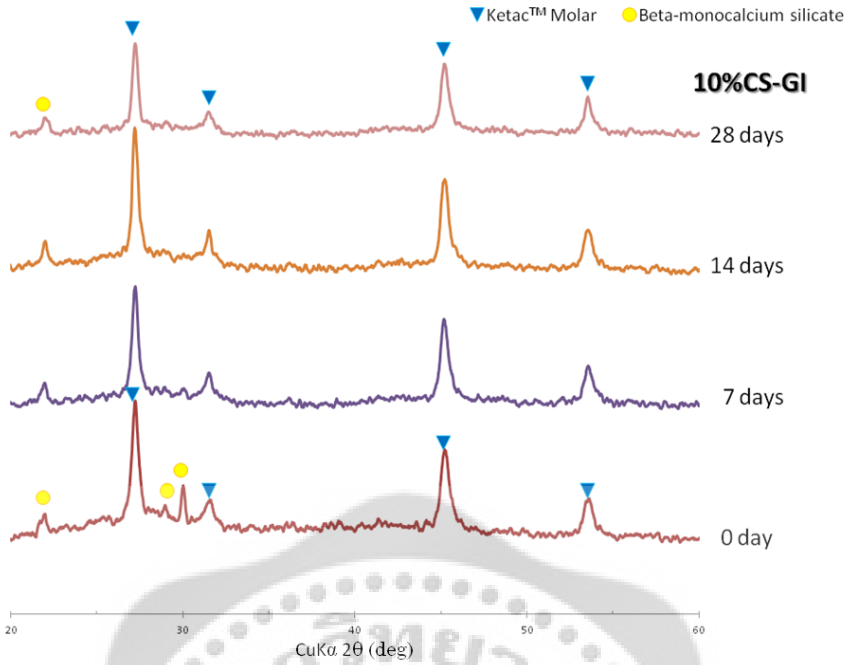

Figure 7 XRD patterns of 10%CS-GI specimens before and after soaking in the SBF for various times (all of 4 peaks of Ketac™ Molar (▼) are observed after soaking in SBF but only one peak of beta-monocalcium silicate (●) remain)

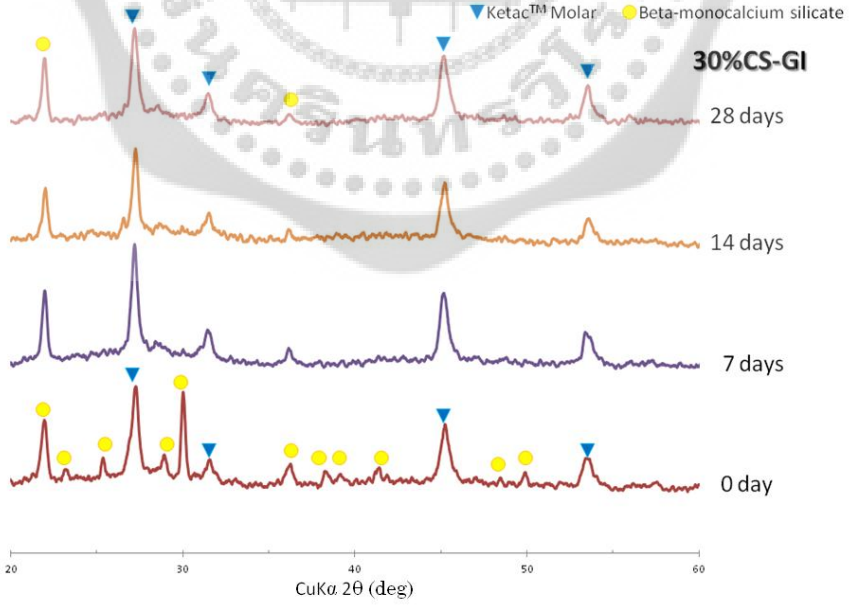

Figure 8 XRD patterns of 30%CS-GI specimens before and after soaking in the SBF for various times (all of 4 peaks of Ketac™ Molar (▼) are observed after soaking in SBF but only two peak of beta-monocalcium silicate (●) remain)

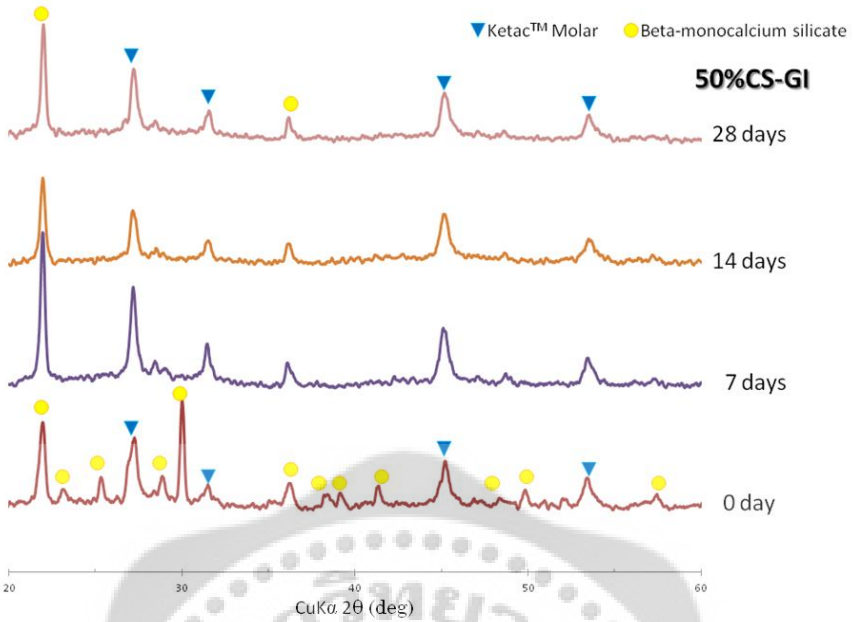

Figure 9 XRD patterns of 50%CS-GI specimens before and after soaking in the SBF for various times (all of 4 peaks of Ketac™ Molar (▼) are observed after soaking in SBF but only two peak of beta-monocalcium silicate (●) remain)

SEM micrograph analysis

Figure 10-14 show the SEM micrographs of the surfaces of specimens of five material groups before and after soaking at magnification 1000X. Figure 15 show the SEM micrographs of 50%CS-GI before and after soaking at magnification 2500X and 5000X, respectively. Apatite-like crystals could be observed on the surfaces of MTA and 50%CS-GI after soaking for 7 days. The amount and size of the deposited crystals were greater when the soaking time was longer.

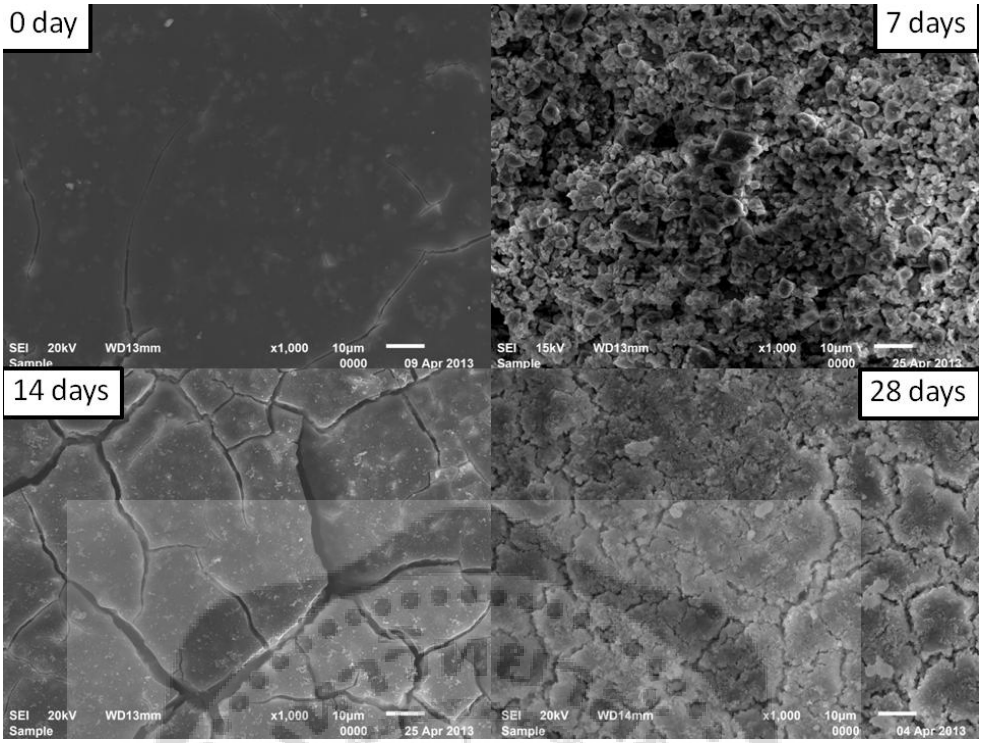

Figure 10 SEM micrographs of the surfaces of GI specimens before and after soaking in the SBF solution for various times

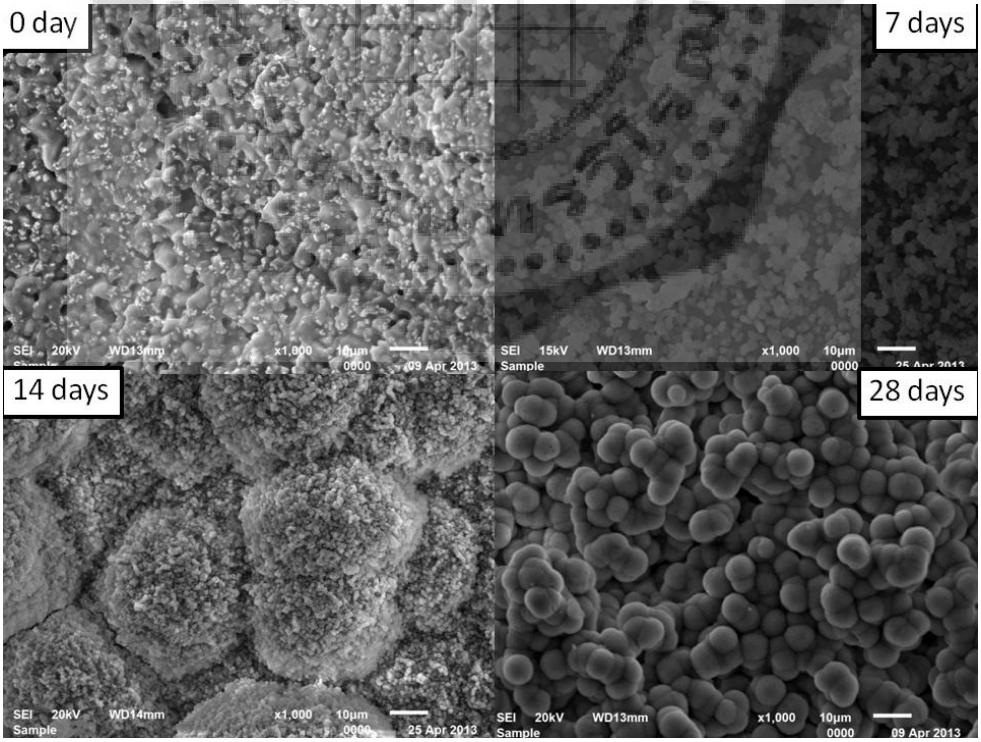

Figure 11 SEM micrographs of the surfaces of MTA specimens before and after soaking in the SBF solution for various times

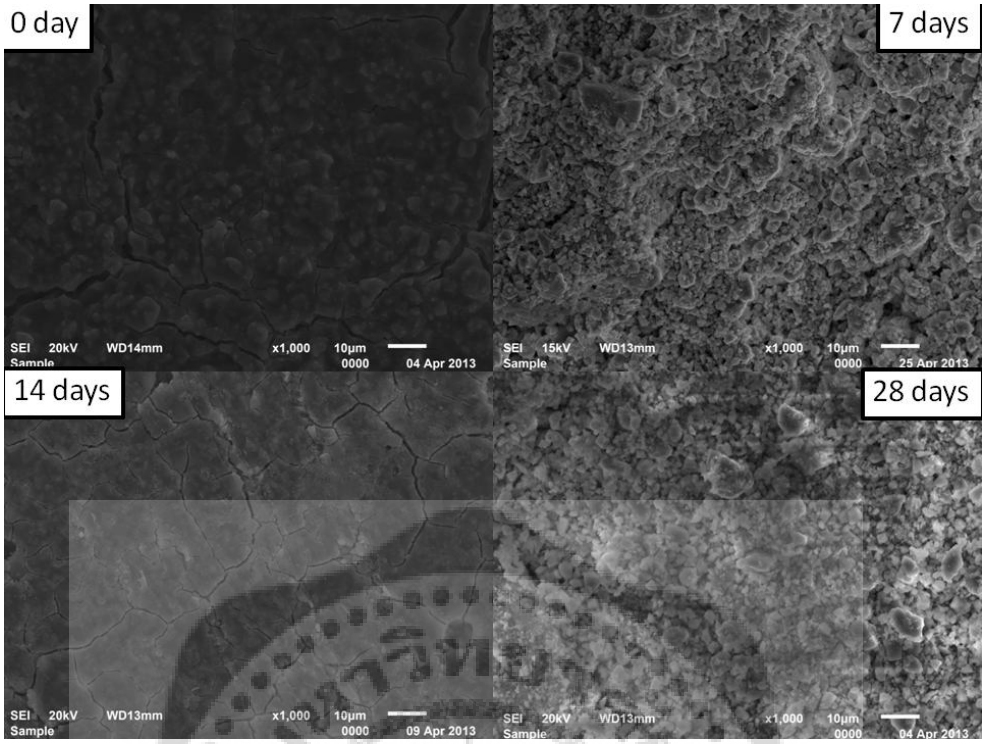

Figure 12 SEM micrographs of the surfaces of 10%CS-GI specimens before and after soaking in the SBF solution for various times

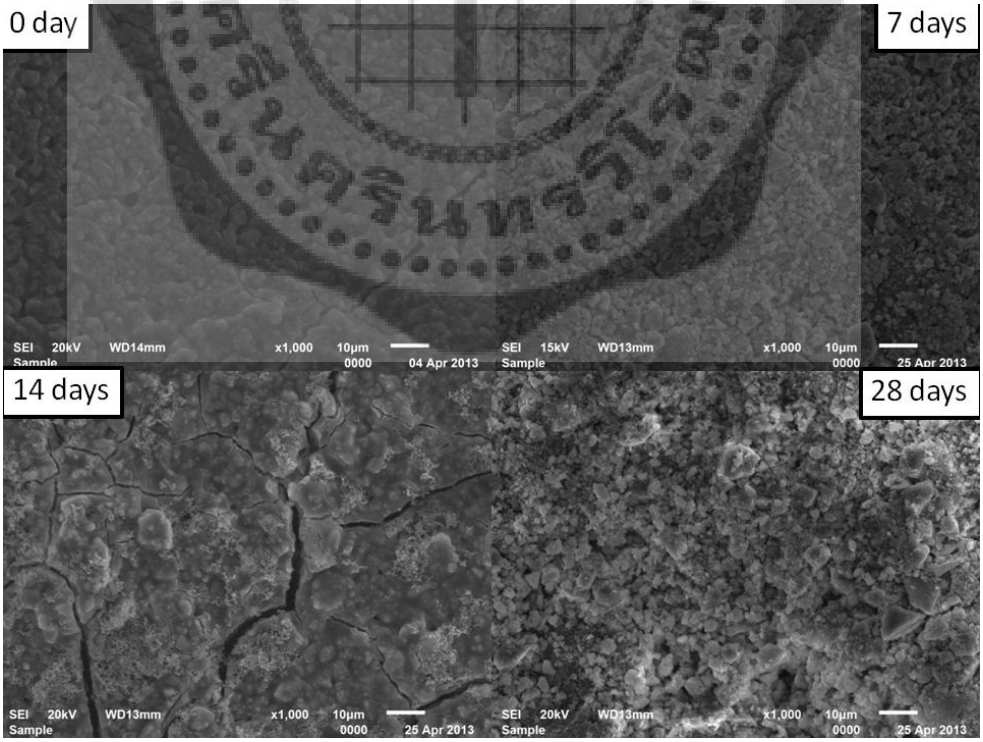

Figure 13 SEM micrographs of the surfaces of 30%CS-GI specimens before and after soaking in the SBF solution for various times

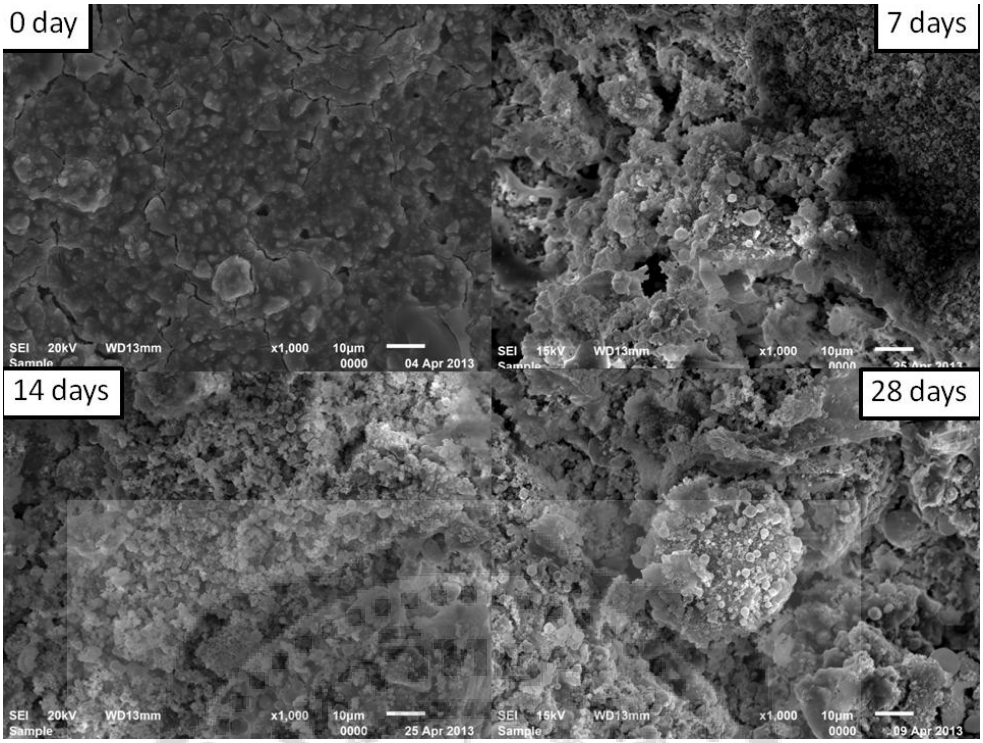

Figure 14 SEM micrographs of the surfaces of 50%CS-GI specimens before and after soaking in the SBF solution for various times

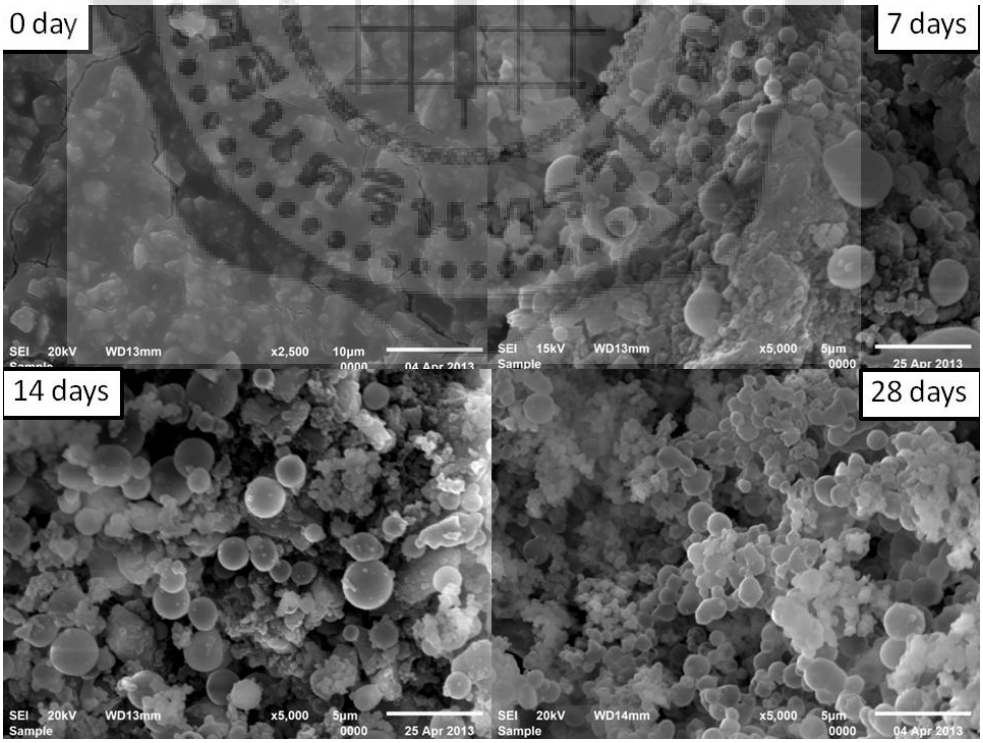

Figure 15 SEM micrographs of the surfaces of 50%CS-GI specimens before and after soaking in the SBF solution for various times at 2500X and 5000X

XRF analysis

To ensure the formation of hydroxyapatite-like crystals in the soaked 50%CS-GI specimens. X-ray fluorescence (XRF) was used to determine the chemical compositions on the surface of all five groups before soaking and 28-day soaking specimen. Weight percent of Ca and P were considered and calculated into molar ratio. The Ca/P molar ratios of all groups are presented in Table 5. The ratios of specimens before soaking were far from 1.67, which represented to hydroxyapatite. However, the ratios of 28-day soaked specimens of other groups were closed to 1.67.

Additionally, Table 6 shows the Ca/P molar ratios of 50%CS-GI groups. The phosphate and calcium ions tend to increase with increasing the soaking time, whereas the silicon ion tends to decrease. Therefore, Ca/P molar ratios of the specimens that soaked for longer time were more closed to 1.67 than those with shorter soaking time.

Table 5 Elemental composition and molar ratios of the surfaces of the materials in comparison before and after soaking in the SBF solution for 28 days

Materials	SBF soaking condition	Elemental composition (Wt%)			Molar ratio of Ca/Si	Molar ratio of Ca/P
		SiO_2	P_2O_5	CaO		
GIC	Before soaking	51.05	9.76	39.20	0.82	4.70
	28days soaking	34.71	31.77	33.51	1.03	1.23
10%CS-GI	Before soaking	61.10	10.52	28.38	0.50	3.15
	28days soaking	48.44	21.89	29.68	0.66	1.59
30%CS-GI	Before soaking	59.00	7.47	33.53	0.61	5.25
	28days soaking	57.18	17.71	25.12	0.47	1.66
50%CS-GI	Before soaking	65.24	6.12	28.64	0.47	5.47
	28days soaking	40.40	23.46	36.14	0.96	1.80
MTA	Before soaking	24.97	2.14	72.89	3.13	39.84
	28days soaking	N/A	23.01	73.4	N/A	1.59

Table 6 Elemental composition and molar ratios of the surfaces of 50%CS-GI specimens in comparison before and after soaking in the SBF solution for various times

	0 day	7 days	14 days	28 days
SiO_2	65.24	69.82	57.07	40.40
P_2O_5	6.12	8.60	17.65	23.46
CaO	28.64	21.58	25.29	36.14
Molar ratio of Ca/Si	0.47	0.33	0.47	0.96
Molar ratio of Ca/P	5.47	2.93	1.68	1.80

Biocompatibility test

MTT assays

The percentages of viable cells exposed to four concentrations of extracts from five groups are shown in Figure 16. The percentage of cell viability exposed to undiluted extracts from GIC (52.65%) was not different from those of 10%CS-GI (75.46%), but significantly lesser than those of 30%CS-GI, 50%CS-GI and MTA (92.47%, 100.77%, and 94.20, respectively). The percentage of cell viability of full concentrated 10%CS-GI group was not different from those of full concentrated 30%CS-GI and MTA, a half concentrated GIC, 30%CS-GI and MTA, and a quarter concentrated MTA.

The percentages of cell viability exposed to 1:1, 1:2 and 1:4 diluted extracts were not significantly different amongst all five groups. The cell viability was likely to depend on extract concentration; the lower concentration, the higher level of cell viability.

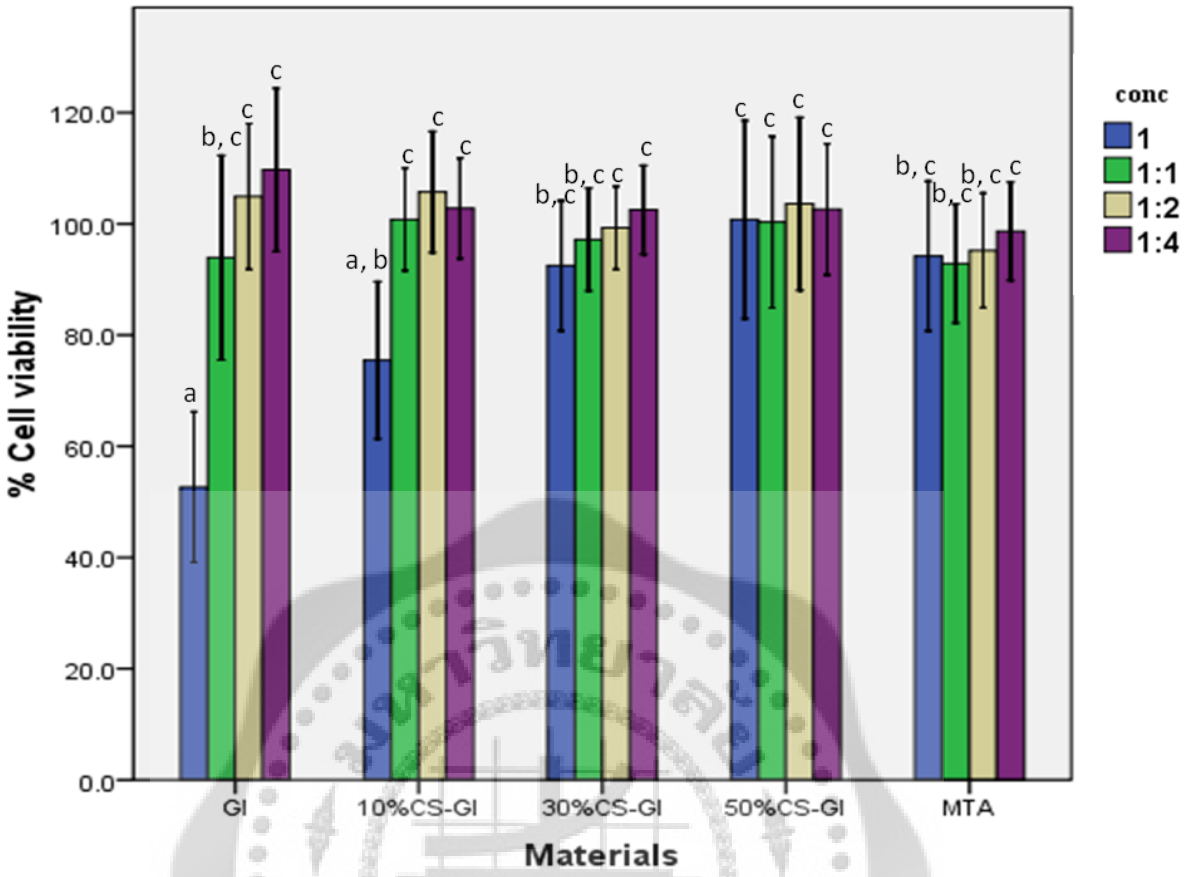

Figure 16 Percentage of cell viability exposed to 4 concentrations of extracts from all groups

Cell morphology

The morphology of PDL fibroblast cells exposed to various concentrations of extracts from all five groups are shown in Figure 17. Most of the cells exposed to undiluted GIC extracts were round-shaped, fewer cytoplasmic extensions and dispersive appearance. Some cells exposed to undiluted 10%CS-GIC extracts were round-shaped like those from GIC groups but the cells were slightly confluent. However, the cells from these groups were more spindles and more confluent when exposed to the more diluted concentrations. Contrarily, most of cells exposed to MTA were spindle-shaped and confluent in all concentrations. The cells exposed to 30%CS-GIC and 50%CS-GIC in all concentrations tended to be spindle-shaped and confluent like those cells from MTA groups.

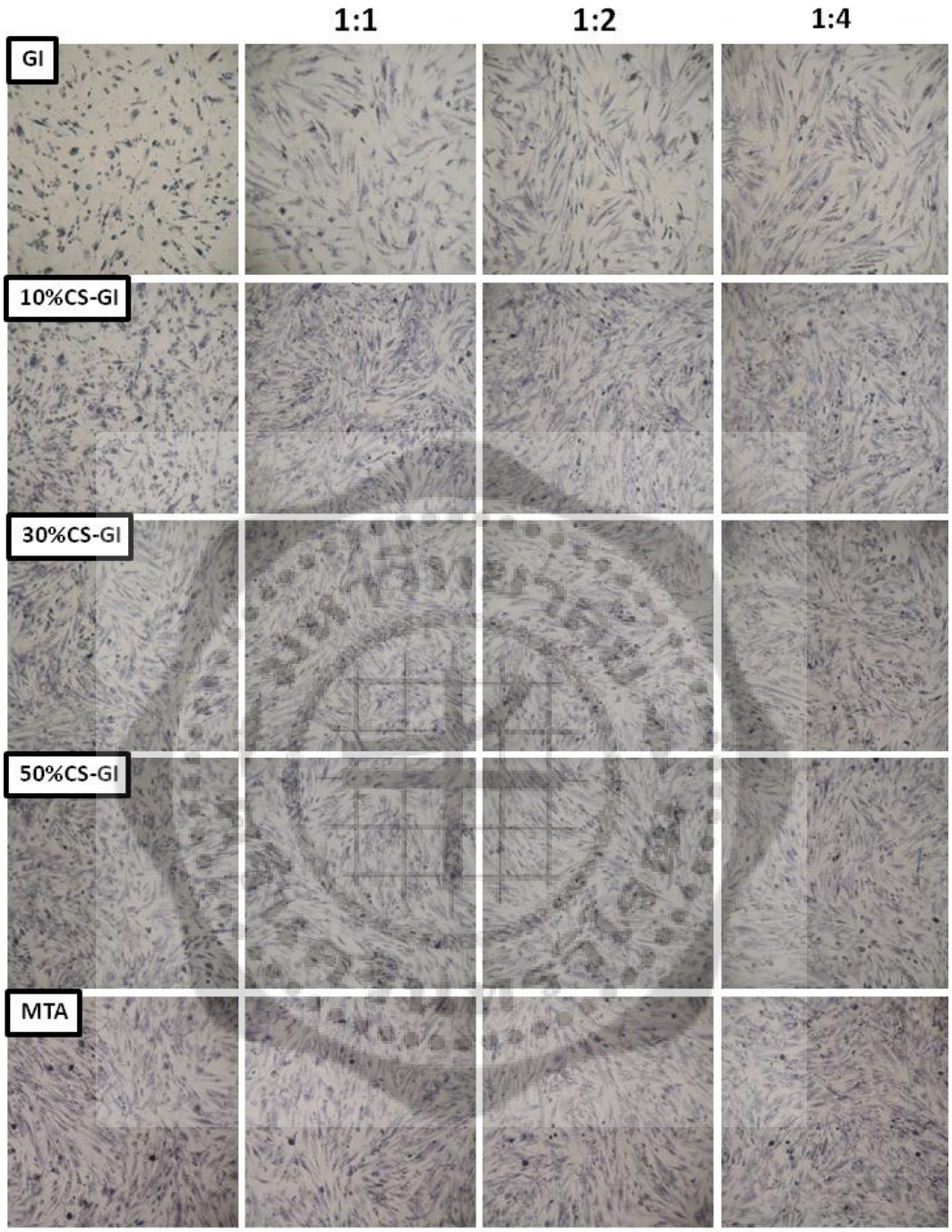

Figure 17 Cell morphology exposed to 4 concentrations of extracts from all five material groups

Chapter 5

Discussion

Improvement in the devices and materials allows the majority of dentists to perform better works. Bioactive materials, firstly aim to place implantation into bone tissue without encapsulated by a fibrous tissue, have been designed for use in medicine and dentistry.[94,115] However, the bioactivity of the materials can be predicted from the apatite formation on its surface in SBF solution.[115]

Beta-monocalcium silicate powder used in this study was prepared by the co-precipitation method according to Siriphannon *et al*. They claimed that the powder could rapidly released calcium ion and silicon ions to simulate body fluid solution, resulting in the formation of hydroxyapatite within 1 day.[12] The growth rate of apatite layers was higher than that found in monocalcium silicate prepared from other methods.[116] However, the characterization of beta-monocalcium silicate used in this study not only showed the pattern of beta-monocalcium silicate itself but also showed that of cristobalite peak (2 theta = 22). The explanation of this result is the beta-monocalcium silicate crystalline grains were surrounded with cristobalite phase.[13] The presence of cristobalite grain boundary could both promote the hydroxyapatite formation and improve the adhesion of hydroxyapatite on the surface of monocalcium silicate.[13]

Altogether the findings from XRD, SEM and XRF, GIC specimens did not show any sign of new hydroxyapatite formation within the 28-day-soaking period. Even though some previous papers claimed that GIC had bioactivity properties,[117] our study found that the GIC lacked of ability to forming hydroxyapatite in SBF solution. The MTA specimens evidently were observed that formation at 7th day after soaking. This result is in agreement with various

researches which reported the bioactivity of MTA immersed in physiological solution.[5,23,42] The key ingredient of MTA is tricalcium silicate, this active component could rapidly react with the phosphate group in the solution to form as hydroxyapatite.

The XRD pattern of the unsoaked specimens of the test groups showed the combination of GIC, cristobalite and beta-monocalcium silicate. After soaking in SBF solution, the peak patterns of beta-monocalcium silicate were reduced, but those of GIC and cristobalite were still remained. This result reflects that crystalline grains of beta-monocalcium silicate could dissolve in the SBF solution but the cristobalite phase at grain boundary unchanged on the sample surface. However, all of three test groups were not present the peak patterns of hydroxyapatite.

The findings from SEM micrographs and XRD patterns of soaked 10%CS-GI and 30%CS-GI specimens did not show any signs of hydroxyapatite formation, but those from XRF investigation concealed that the Ca/P molar ratios of 28-day-soaking of both groups were closed to the hydroxyapatite theortetical ratio. However, we scarcely believed that the crystals were formed. Polyacrylic acid, resin binder of Ketac™ Molar, might hinder the apatite forming.[27, 28] Our result was in agreement with Yli-Urpo *et al*[24] who suggested that the composites of conventional GIC (Fuji II, GC Corp) and 30%wt Bioactive glass (BAG) did not clearly observe the apatite formation using SEM analysis in 336-hour-soaked specimen. Contrarily, soaked 50%CS-GI not only revealed the hydroxyapatite crystals under SEM but the Ca/P ratio of 14- and 28-day-soaking were also closed to hydroxyapatite ratio. Although the XRD pattern did not show any peaks corresponding to hydroxyapatite even after prolong soaking for 28 days, we believed that the hydroxyapatite crystals were formed but the nucleated size of them were relatively small with thin layer that not enough to conceal the XRD signals, but could revealed the SEM and XRF signals, more superficially detected than XRD.

Altogether, these data indicated that the 50% CS-GI specimens soaked in the SBF solution at least 7 days could induce the apatite formation on their surfaces, implying to its bioactivity. The explanation of this result is that the number of beta-monocalcium silicate powder was high enough to spread thoroughly on the surface of specimen, so the new hydroxyapatite could completely deposit over the surface. Moreover, the volume of added monocalcium silicate powder, slightly basic pH,[110] adequate to overcome the effect of polyacrylic acid that could neutralize the acidic pH of GIC and facilitate the hydroxyapatite formation.

Biocompatibility is a crucial property in medical and dental materials that is contacted or implanted in human tissues. In our study, the MTT assay was used to measure the cytotoxicity of all materials because the method is not expensive, easy to test and reliability[118]. The specimen preparation followed ISO 10993-12:2007 standard,[119] and the test protocol followed ISO 10993-5:2009 for *in vitro* cytotoxicity test.[120] We used human periodontal ligament fibroblast cell instead of immortalized fibroblast cells to simulate the *in vivo* situation. In addition, we also assessed cell morphology because the alteration of cellular morphology could depict the physiological state of the cells.

In our study, the percentages of viable PDL fibroblast cells exposed to undiluted extracts from Ketac™ Molar and 10%CS-GI groups were significantly lower than other groups. Our result is strongly consistent with Vajrabhaya *et al*[22] who investigated the cytotoxicity of MTA and Ketac™ Molar and demonstrated that the inhibition of PDL cell proliferation by the extracts of Ketac™ Molar was significantly greater than that of MTA. Abdullah *et al*[54] also reported that SaOs-2 osteosarcoma cell was round morphology and not able to adhere to GIC's surface but there was an increase in cell number adhering to MTA's surface. An explanation for our result could come from the leachable compounds of MTA and GIC. The calcium ion released during setting reaction of MTA played a role in proliferation, differentiation and maturation of osteogenic cells,[98] while Al^{3+}, F^{-}, Si^{-} and

unpolymerized acid are mainly leachable compounds of GIC that might affect the cells and tissues. Many previous studies have expressed of the toxicity of the released components. Savarino *et al*[121] reported that the release of fluoride and aluminium ions in early setting reaction combined with acidity made the GIC toxic. Consiglio *et al*[122] also found that released fluoride ions and acidic pH of GIC inhibited protein synthesis of human gingival fibroblast.

The cytotoxic level of 30%CS-GI and 50%CS-GI groups were similar to that of MTA. The adding of monocalcium silicate powder could neutralize the acidic pH from GIC by-product and stabilize the pH of the DMEM in optimal range for cell survivals. Moreover, calcium ions released from beta-monocalcium silicate might facilitate the viability of the cell as well. For all of these reasons, adding $CaSiO_3$ to GIC could reduce the toxicity of GIC.

In the present study, the percentages of viable cells exposed to any diluted extracts from all groups were not significantly different. Moreover, the cytotoxic level was prone to adversely proportional to the concentration, which associated with the amount of leachable compound. The higher amount of toxic leachants, the more acidic pH of the solution. This lead to the cell damage and death.

Based on the findings obtained in the present investigation, we concluded that adding beta-monocalcium silicate more than 30% by weight to GIC could increase biocompatibility of GIC, while adding beta-monocalcium silicate more than 50% by weight to GIC could have bioactivity. The formed hydroxyapatite previously claimed to enhance the leakage resistance as well. Therefore, for further study, it is important to examine the leakage properties of 50%CS-GI sample.

REFERENCES

REFERENCES

1. Roberts HW, Toth JM, Berzins DW, Charlton DG. Mineral trioxide aggregate material use in endodontic treatment: A review of literature. Dent Mater 2008;24:149-64.

2. Torabinejad M, Parirokh M. Mineral trioxide aggregate: a comprehensive literature review – part I: chemical, physical and antibacterial properties. J Endod 2010;36:16-27.

3. Torabinejad M, Parirokh M. Mineral trioxide aggregate: a comprehensive literature review – part II: leakage and biocompatibility investigations. J Endod 2010;36:190–202.

4. Torabinejad M, Parirokh M. Mineral trioxide aggregate: a comprehensive literature review – part III: clinical applications, drawbacks, and mechanism of action. J Endod 2010;36:400-13.

5. Sarkar NK, Caicedo R, Ritwik P, Moiseyeva R, Kawashima I. Physicochemical basis of the biologic properties of mineral trioxide aggregate. J Endod 2005;31:97–100.

6. Zhao WY, Wang JY, Zhai WY, Wang Z, Chang J. The self-setting properties and in vitro bioactivity of tricalcium silicate. Biomaterials 2005;26:6113–21.

7. Gou Z, Chang J. Synthesis and in vitro bioactivity of dicalcium silicate powder. J Euro Ceram Soc 2004;24:93-9.

8. Liu WN, Chang J, Zhu YQ, Zhang M. Effect of tricalcium aluminate on the properties of tricalcium silicate-tricalcium aluminate mixtures: setting time, mechanical strength and biocompatibility. Int Endod J 2011;44:41-50.

9. Huan Z, Chang J. Self-setting properties and in vitro bioactivity of calcium sulfate hemihydrates-tricalcium silicate composite bone cements. Acta Biomaterialia 2007;3:952-60.

10. Huan Z, Chang J, Huang XH.Self-setting properties and in vitro bioacativity of $Ca_2SiO_4/CaSO_4 \cdot 1/2H_2O$ composite bone cement. J Biomed Mater Res B Appl Biomater 2008;87:387-94.

11. Siriphannon P, Hayashi S, Yasumori A, Okada K. Preparation and sintering of $CaSiO_3$ from coprecipitated powder using NaOH as precipitant and its apatite formation in simulated body fluid. J Mater Res 1999;14:529–536.

12. Siriphannon P, Kameshima Y, Yasunori a, Okada K, Hayashi S. Influence of preparation conditions on the microstructure and bioactivity of α-$CaSiO_3$ ceramics; formation of hydroxyapatite in simulated body fluid. J Biomed Mater Res 2000;52:30-9.

13. Siriphannon P, Kameshima Y, Yasumori A, Okada K, Hayashi S. Formation of hydroxyapatite on $CaSiO_3$ powders in simulated body fluid, J Eur Ceram Soc 2002;22:511–520.

14. Hazar BY. Preparation and in vitro bioactivity of $CaSiO_3$ powders. Ceram Int 2007;33:687-92.

15. De Aza PN, Luklinska ZB, Anseau MR, Guitian F, De Aza S. Bioactivity of pseudowollastonite in human saliva. J Dent 1999;27:107–113.

16. Wei J, Chen F, Shin JW, Hong H, Dai C, Su J, Liu C. Preparation and characterization of bioactive mesoporous wollastonite – polycaprolactone composite scaffold. Biomaterials 2009;30:1080-8.

17. Hosoya Y, Garcia-Godoy F. Bonding mechanism of Ketac-molar aplicap and Fuji IX GP to enamel and dentin. Am J Dent 1998;11:235–9.

18. Davidson CL. Advances in glass-ionomer cements. Chicago, USA: Quintessence Pub. Co.;1999.

19. Mount G. Glass-ionomer cements: past, present and future. Oper Dent 1994;19:82–90.

20. Nagaraja Upadhya P, Kishore G. Glass ionomer cement – the different generations. Trends Biomater Artif Organs 2005;18:158-65.

21. Costa C, Hebling J, Garcia-Godoy F, Hanks C. In vitro cytotoxicity of glass-ionomer cements. Biomaterials 2003;24:3853-8.

22. Vajrabhaya L, Korsuwannawong S, Jantarat J, Korre S. Biocompatibility of furcal perforation repair material using cell culture technique: Ketac Molar versus ProRoot MTA. Oral Surg Oral Med Oral Pathol Oral Radiol Endod 2006;102:e48-50.

23. Bozeman TB, Lemon RR, Eleazer PD. Elemental analysis of crystal precipitate from gray and white MTA. J Endod 2006;32:425–8.

24. Yli-Urpo H, Lassila LVJ, Narhi T, Vallitu PK. Compressive strength and surface characterization of glass ionomer cements modified by particles of bioactive glass. Dent Mater 2005;21:201-9.

25. Loof J, Svahn F, Jarmar T, Engqvist H, Pameijer CH. A comparative study of the bioactivity of three materials for dental applications. Dent Mater 2008;24:653-9.

26. Arita K, Yamamoto A, Shinonaga Y, Harada K, Abe Y, Nakagawa K, Sugiyama S. Hydroxyapatite particle characteristics influence the enhancement of the mechanical and chemical properties of conventional restorative glass ionomer cement. Dent Mater J 2011;30:672-83.

27. Kamitakahara M, Kawashita M, Kokubo T, Nakamura T. Effect of polyacrylic acid on the apatite formatioin of a bioactive ceramic in a simulated body fluid: fundamental examination of the possibility of obtaining bioactive glass-ionomer cements for orthopaedic use. Biomaterials 2001;22:3191-6.

28. Matsuya S, Matsuya Y, Ohta M. Structure of bioactive glass and its application to galss-ionomer cement. Dent Mater J 1999;18:155-66.

29.Torabinejad M, Watson TF, Pitt Ford TR. Sealing ability of a mineral trioxide aggregate when used as a root end filling material. J Endod 1993;19:591–5.

30. United States Patent 5,415,547, Torabinejad M, White Dean J; May 16, 1995.

31. PROROOT MTA, Product Literature, Dentsply Tulsa Dental, Tulsa, OK 74136.

32. Taylor HFW. Cement chemistry. 2nd ed. London: Thomas Telford; 1997: 1–28.

33. Camilleri J, Montesin FE, Brady K, Sweeney R, Curtis RV, Pitt Ford TR. The constitution of mineral trioxide aggregate. Dent Mater 2005;21:297–303.

34. Camilleri J, Pitt Ford TR. Mineral trioxide aggregate: a review of the constituents and biological properties of the material. Int Endod J 2006;39:747–54.

35. Asgary S, Parirokh M, Eghbal MJ, Brink F. Chemical difference between white and grey mineral trioxide aggregate. J Endod 2005;31:101-3.

36.Song JS, Mante FK, Romanow WJ, Kim S. Chemical analysis of powder and set forms of Portland cement, gray ProRoot MTA, white ProRoot MTA, and gray MTA-Angelus. Oral Surg Oral Med Oral Pathol Oral Radiol Endod 2006;102:809-15.

37.BelÍo-Reyes IA, Bucio L, Cruz-Charvez E. Phase Composition of ProRoot Mineral Trioxide Aggregate by X-Ray Powder Diffraction. J Endod 2009;35:875-8.

38.Dammaschke T, Gerth HUV, Züchner H, Schäfer E. Chemical and physical surface and bulk material characterization of white ProRoot MTA and two Portland cements. Dent Mater 2005;21:731-8.

39. Camilleri J. Hydration reaction of mineral trioxide aggregate. Int Endod J 2007;40:462-70.

40. Dunstetter F, de Noirfontaine MN, Courtial M. Polymorphism of tricalcium silicate, the major compound of Portland cement clinker 1: structural data—review and unified analysis. Cement Concrete Res 2006;36:39–53.

41. Stanek T, Sulovsky. The influence of the alite polymorphism on the strength of the Portland cement. Cement Concrete Res 2002;32:1169–75.

42.Tay FR, Pashley DH, Rueggeberg FA, Loushine RJ, Weller RN, Calcium phosphate phase transformation produced by the interaction of the Portland cement component of white mineral trioxide aggregate with a phosphate-containing fluid. J Endod 2007;33:1347–51.

43. Gandolfi MG, Pagani S, Perut F, Ciapetti G, Baldini N, Mongiorgi R, et al. Innovative silicate-based cements for endodontics: a study of osteoblast-like cell response. J Biomed Mater Res 2008;87A:477–86.

44. Gandolfi MG, Van Landuyt K, Taddei P, Modena E, Van Meerbeek B, Prati C. ESEM–EDX and Raman techniques to study ProRoot MTA and calcium-silicate cements in wet conditions and in real-time. J Endod 2010;36:851–7.

45.Gandolfi MG, Taddei P, Siboni F, Modena E, Ciapetti G, Prati C. Development of the foremost light-curable calcium-silicate MTA cement as root-end in oral surgery. Chemical–physical properties, bioactivity and biological behavior. Dent Mater 2010;27:e134-57.

46. Tang HM, Torabinejad M, Kettering JD, Leakage Evaluation of Root End Filling Materials Using Endotoxin. J Endod 2002; 28: 5-7.

47. Martin RL, Monticelli F, Brackett WW, Loushine RJ, Rockman RA, Ferrari M, Pashley DH, Tay FR. Sealing properties of mineral trioxide aggregate orthograde apical plugs and root fillings in an in vitro apexification model. J Endod 2007;33:272-5.

48. Reyes-Carmona JF, Felippe MS, Felippe WT, Biomineralization Ability and Interaction of Mineral Trioxide Aggregate and White Portland Cement With Dentin in a Phosphate-containing Fluid. J Endod 2009;35:731–6.

49. Reyes-Carmona JF, Felippe MS, Felippe WT. A Phosphate-buffered Saline Intracanal Dressing Improves the Biomineralization Ability of Mineral Trioxide Aggregate Apical Plugs. J Endod 2010;36:1648–1652.

50. Balto HA. Attachment and Morphological Behavior of Human Periodontal Ligament Fibroblasts to Mineral Trioxide Aggregate: A Scanning Electron Microscope Study. J Endod 2004; 30: 25-9.

51. AL-rabeah E, Peripanayagam H, MacFarland D. Human alveolar bone cells interact with ProRoot and tooth-colored MTA. J Endod 2006;32:872-5.

52.Paranjpe A, Zhang H, Johnson JD. Effects of mineral trioxide aggregate on human dental pulp cells after pulp-capping procedures. J Endod 2010;36:1042–1047.

53. Thomson TS, Berry JE, Somerman MJ, Kirkwood KL. Cementoblasts maintain expression of osteocalcin in the presence of mineral trioxide aggregate. J Endod 2003;29:407–12.

54. Abdullah D, Pitt Ford TR, Papaioannou S, Nicholson J, McDonald F. An evaluation of accelerated Portland cement as a restorative material. Biomaterials 2002;23:4001-10.

55. Keiser K, Johnson CC, Tipton DA. Cytotoxicity of mineral trioxide aggregate using human periodontal ligament fibroblasts. J Endod 2000;26:288-91.

56. Koulaouzidou EA, Papazisis KT, Economides NA, Beltes P, Kortsaris AH. Antiproliferative effect of mineral trioxide aggregate, zinc oxide-eugenol cement and glass-ionomer cement against three fibroblastic cell lines. J Endod 2005;31:44-6.

57. Osorio RM, Hefti A, Vertucci FJ, Shawley AL. Cytotoxicity of endodontic materials. J Endodontics 1998;24:91–6.

58. Saidon J, He J, Zhu Q, Safavi K, Spangberg LS. Cell and tissue reactions to mineral trioxide aggregate and Portland cement. Oral Surg Oral Med Oral Pathol Oral Radiol Endod 2003;95:483–9.

59. Bonson S, Jeansonne BG, Lallier TE. Root-end filling materials alter fibroblast differentiation. J Dent Res 2004;83:408–13.

60. Hakki SS, Bozkurt SB, Hakki EE, Belli S. Effects of mineral trioxide aggregate on cell survival, gene expression associated with mineralized tissues, and biomineralization of cementoblasts. J Endod 2009;35:513-9.

61. Yasuda Y, Ogawa M, Arakawa T, Kadowaki T, Saito T. The effect of mineral trioxide aggregate on the mineralization ability of rat dental pulp cells: an in vitro study. J Endod 2008;34:1057–60.

62. Maeda H, Nakano T, Tomokiyo A, Fujii S, Wada N, Monnouchi S, Hori K, Akamine A. Mineral trioxide aggregate induces bone morphogenetic protein-2 expression and calcification in human periodontal ligament cells. J Endod 2010;36:647-52.

63. Takita T, Hayashi M, Takeichi O, Ogiso B, Suzuki N, Otsuka K, Ito K. Effect of mineral trioxide aggregate on proliferation of cultured human dental pulp cells. Int Endod J 2006;39:415–22.

64. Tani-Ishii N, Hamada N, Watanabe K, Tujimoto Y, Teranaka T, Umemoto T. Expression of bone extracellular matrix proteins on osteoblast cells in the presence of mineral trioxide. J Endod 2007;33:836–9.

65. Nakayama A, Ogiso B, Tanabe N, Takeichi O, Matsuzaka K, Inoue T. Behaviour of bone marrow osteoblast-like cells on mineral trioxide aggregate: morphology and expression of type I collagen and bone-related protein mRNAs. Int Endod J 2005;38:203–10.

66. Parirokh M, Mirsoltani B, Raoof M, Tabrizchi H, Haghdoost AA. Comparative study of subcutaneous tissue responses to a novel root-end filling material and white and grey mineral trioxide aggregate. Int Endod J 2010;44:283-9.

67. Baek SH, Plenk H, Kim S. periapical tissue response and cementum regeneration with amalgam, superEBA and MTA as root-end filling materials. J Endod 2005;31:444-9.

68. Sousa CJA, Loyola AM, Versiani MA, Biffi JCG, Oliveira RP, Pascon EA. A comparative histological evaluation of the biocompatibility of the materials used in apical surgery. Int Endod J 2004;37:738-48.

69. Yaltirik M, Ozbas H, Bilgic B, Issever H. Reactions of connective tissue to mineral trioxide aggregate and amalgam. J Endod 2004;30:95–9.

70. Zarrabi MH, Javidi M, Jafarian AH, Joushan B. Histologic Assessment of Human Pulp Response to Capping with Mineral Trioxide Aggregate and a Novel Endodontic Cement. J Endod 2010;36:1778-81.

71. Economides N, Pantelidou O, Kokkas A, Tziafas D. Short-term periradicular tissue response to mineral trioxide aggregate (MTA) as root-end filling material. Int Endod J 2003;36:44–8.

72. Holland R, Filho JA, de Souza V, Nery MJ, Bernabe PF, Junior ED. Mineral trioxide aggregate repair of lateral root perforations. J Endod 2001;27:281–4.

73. Regan JD, Gutmann JL, Witherspoon DE. Comparison of Diaket and MTA when used as root-end filling materials to support regeneration of the periradicular tissues. Int Endod J 2002;35:840–7.

74. Apaydin ES, Shabahang S, Torabinejad M. Hard-tissue healing after application of fresh or set MTA as root-end-filling material. J Endod 2004;30:21– 4.

75. Main C, Mirzayan N, Shabahang S, Torabinejad M. Repair of root perforations using mineral trioxide aggregate: a long-term study. J Endod 2004;30:80 –3.

76. Pace R, Giuliani V, Pagavino G. Mineral trioxide aggregate as repair material for furcal perforation: case series. J Endod 2008;34:1130–3.

77. de Chevigny C, Dao TT, Basrani BR, et al. Treatment outcome in endodontics: the Toronto study—phases 3 and 4: orthograde retreatment. J Endod 2008;34:131–7.

78. Torabinejad M, Hong CU, McDonald F, Pitt Ford TR. Physical and chemical properties of a new root-end filling material. J Endod 1995;21:349-53.

79. Lohbauer U. Dental glass ionomer cement as permanent filling materials? – properties, limitations and future trends. Materials 2010;3:76-96.

80. Zimehl R, Hannig M. Non metallic restorative materials based on glass ionomer cements – recent trends and developments. Colloids and surfaces A : Physicochem Eng Aspect 2000;163:55-62.

81. Xie D, Brantley WA, Culbertson BM, Wang G. Mechanical properties and microstructures of glass-ionomer cements. Dent Mater 2000;16:129-38.

82. Kilpatrick NM, Murray JJ, McCabe JF. The use of a reinforced glass-ionomer cement for the restoration of primary molars: A clinical trial. Br Dent J 1995;179:175-9.

83. Sarkar NK. Metal-matrix interface in reinforced glass-ionomers. Dent Mater 1999;15:421-5.

84. Williams JA, Billington RW, Pearson G. Silver and fluoride release from metal-reinforced glass-ionomer filling materials. J Oral Rehabil 1997;24:369-75.

85. Guggenberger R, May R, Stefan KP. New trends in glass-ionomer chemistry. Biomaterials 1998;19:479-83.

86. Product Dossier, Ketac Molar, 3M ESPE.

87. Stamboulis A, Law RV, Hill RG. Characterisation of commercial ionomer glasses using magic angle nuclear magnetic resonance (MAS-NMR). Biomaterials 2004;25:3907-13.

88. Peez R, Frank S. The physical-mechanical performance of the new Ketac™ Molar Easymix compared to commercially available glass ionomer restoratives. J Dent 2006;34:582-7.

89. Sengun A, Botsali HE, Yalcin M, Ozer F, Tasdemir ST, Hakki SS. Evaluation of cytotoxicity of glass ionomer cements by dentin barrier test. Dent Mater 2009 (Abstract);25:e39.

90. Leyhausen G, Abtahi M, Karbakhsch M, Sapotnick A, Geurtsen W. The biocompatibility of various resin-modified and one conventional glass-ionomer cement. Biomaterials 1998;19:559–64.

91. Oliva A, Ragione D, Salerno A, Riccio V, Tartaro G, Gozzolino A. Biocompatibility studies on glass ionomer cements by primary cultures of human osteoblasts. Biomaterials 1996;17:1351–6.

92. Geurtsen W, Spahl W, Leyhausen G. Residual monomer/additive release and variability in cytotoxicity of light-curing glassionomer cements and compomers. J Dent Res 1989;77:2012–9.

93. Chong BS, Pitt Ford TR, Kariyawasam SP. Short-term tissue resoponse to potential root-end filling materials in infected root canals. Int Endod J 1997;30:240-9.

94. Heness G, Ben-Nissan B. Innovative bioceramics. Materials Forum 2004;27:104-14.

95. Hoppe A, Guldal NS, Boccaccini AR. A review of the biological response to ionic dissolution products from bioactive glasses and glass-ceramics. Biomaterials 2011;32:2757-74.

96. Ehara A, ogata K, Imazato S, Ebisu S, Nakano T, Umakoshi Y. Effects of alpha TCP and TetCP on MC3T3-E1 proliferation, differentation and mineralization. Biomaterials 2003;24:831-6.

97.Okuda T, Ioku K, Yonezawa I, Minagi H, Kawachi G, Gonda Y, et al. The effect of the microstructure of beta-tricalcium phosphate on the metabolism of subsequently formed bone tissue. Biomaterials 2007;28:2612-21.

98. Maeno S, Niki Y, Matsumoto H, Morioka H, Yatabe T, Funayama A, et al. The effect of calcium ion concentration on sosteoblast viability, proliferation and differentiation in monolayer and 3D culture. Biomaterials 2005;26:4847-55.

99. Xynos ID, Edgar AJ, Buttery LDK, Hench LL, Polak JM. Ionic products of bioactive glass dissolution increase proliferation of human osteoblasts and induce insulin-like growth factor II mRNA expression and protein synthesis. Biochem Biophys Res Commun 2000;276:461-5.

100. Tsigkou O, Jones JR, Polak JM, StevensMM. Differentiationof fetal osteoblasts and formation of mineralized bone nodules by 45S5Bioglass (R) conditioned medium in the absence of osteogenic supplements. Biomaterials 2009;30:3542-50.

101. Gough JE, Jones JR, Hench LL. Nodule formation and mineralisation of human primary osteoblasts cultured on a porous bioactive glass scaffold. Biomaterials 2004;25:2039-46.

102. Valerio P, Pereira MM, Goes AM, Leite MF. The effect of ionic products from bioactive glass dissolution on osteoblast proliferation and collagen production. Biomaterials 2004;25:2941-8.

103. Kim M-H, Bae Y-J, Choi M-K, Chung Y-S. Silicon supplementation improves the bone mineral density of calcium-deficient ovariectomized rats by reducing bone resorption. Biol Trace Elem Res 2009;128:239-47.

104. Ransinchung GD, Kumar B, Kumar V. Assessment of water absorption and chloride ion penetration of pavement quality concrete admixed with wollastonite and microsilica. Constr Build mater 2009;23:1168-77.

105. Ortega-Lara W, Cortes-Hernandez DA, Best S, Brooks R, Hernandez-Ramirez A. Antibacterial properties, in vitro bioactivity and cell proliferation of titania-wollastonite composites. Ceram Int 2010;36:513-9.

106. Lin K, Chang J, Zeng Y, Qian W. Preparation of macroporous calcium silicate cement. Material Letters 2004;58:2109-13.

107. Lin K, Zhai W, Ni S, Chang J, Zheng Y, Qian W. Study of mechanical property and in vitro biocompatibility of $CaSiO_3$ ceramics. Ceram Int 2005;31:323-6.

108. Ni S, Chang J, Chou L. A novel bioactive porous $CaSiO_3$ scaffold for bone tissue engineering. J Biomed Mater Res A 2006;76A:196-205.

109. De Aza PN, Luklinska ZB, Martinez A, Anseau MR, Guitian F, De Aza S. Morphological and structural study of pseudowollastonite implants in bone. J Microsc 2000;197:60-7.

110. Li H, Chang J. Fabrication and characterization of bioactive wollastonite/PHBV composite scaffold. Biomaterials 2004;25:5473-80.

111. Li H, Chang J. In vitro degradation of porous degradable and bioactive wollastonite/PHBV composite scaffolds. Polymer Degrad Stab 2005;87:301-7.

112. Pattanayak DK. Apatite wollastonite-poly methyl methacrylate bio-composites. Mater Sci Eng 2009;29:1709-14.

113. Monvisade P, Siriphannon P, Jermsungnern R, Rattanabodee S. Preparation of hydroxyapatite/poly(methyl methacrylate) and calcium silicate/poly(methyl methacrylate) interpenetrating hybrid composites. J Mater Sci 2007; 18: 1955-9.

114. Kokubo T, Ito S, Huang ZR, Hayashi T, Sakka S, Kitsugi T, Yamamuro T. Ca,P-rich layer formed on high-strength bioactive glass-ceramic A-W. J Biomed Mater Res 1990;24:331–343.

115. Kokubo T, Takadama H. How useful is SBF in predicting in vivo bone bioactivity. Biomaterials 2006;27:2907-15.

116. Ilmori Y, Kameshima Y, Yasumori A, Okada K. Effects of solid/solution ratio on apatite formation from CaSiO3 ceramics in simulated body fluid. J Mater Sci: Mat Med 2004;15:1247-53.

117. Brook IM, Hatton PV. Glass-ionomers: bioactive implant materials. Biomaterials 1998; 19: 565-71.

118. Mosmann T. Rapid colorimetric assay for cellular growth and survival: application to proliferation and cytoxicity assays. J Immunol Methods 1983;65:55-63.

119. International Standards Organization. Biological evaluation of medical devices - Part 12: sample preparation and reference materials. Switzerland: ISO 10993-12. 2007;1-17.

120. International Standards Organization. Biological evaluation of medical devices - Part 5: tests for in vitro cytotoxicity. Switzerland: ISO 10993-5. 2009;1-34.

121. Savarino L, Cervellati M, Stea S, et al. In vitro investigation of aluminium and fluoride release from compomers, conventional and resin-modified glass-ionomer cements: a standardized approach. J Biomater Sci Polymer Ed 2000; 11: 289-300.

122. Consiglio R, Rengo S, Liguoro D, et al. Inhibition by glass-ionomer cements of protein synthesis by human gingival fibroblasts in continuous culture. Arch Oral Biol 1998; 43: 65-71.

APPENDIX

APPENDIX

Weight percentage and atomic percentage of elemental compositions of GIC specimen analysed by XRF

Oxide:	Net	Wt%	At%	I-Error%
Al_2O_3	20.17	18.3267	16.97	2.45
SiO_2	42.01	24.1664	37.96	1.62
P_2O_5	11.64	4.6182	3.07	3.48
CaO	280.05	18.5558	31.23	0.6
La_2O_3	267.73	32.6532	9.46	0.62
Cr_2O_3	19.82	0.9658	0.6	2.68
MnO	7.63	0.284	0.38	5.23
Fe_2O_3	4.86	0.1869	0.11	7.62
SrO	10.46	0.243	0.22	5.81

Weight percentage and atomic percentage of elemental compositions of 28-day-soaked GIC specimen analysed by XRF

Oxide:	Net	Wt%	At%	I-Error%
Al_2O_3	31.7	16.7633	15.25	1.89
SiO_2	59.84	20.8434	32.19	1.34
P_2O_5	79.29	19.08	12.47	1.15
CaO	465.78	20.124	33.29	0.47
La_2O_3	287.73	22.6089	6.44	0.6
Cr_2O_3	19.46	0.5805	0.35	2.69

Weight percentage and atomic percentage of elemental compositions of 10%CS-GI specimen analysed by XRF

Oxide:	Net	Wt%	At%	I-Error%
Al_2O_3	33.19	17.659	14.63	1.87
SiO_2	103.79	35.6368	50.09	1.01
P_2O_5	23.75	6.138	3.65	2.27
CaO	395.3	16.5535	24.93	0.51
La_2O_3	313.59	22.973	5.95	0.57
Cr_2O_3	21.51	0.6198	0.34	2.55
MnO	9.8	0.2009	0.24	4.34
Fe_2O_3	2.43	0.0504	0.03	13.82
SrO	13.72	0.1686	0.14	4.82

Weight percentage and atomic percentage of elemental compositions of 28-day-soaked 10%CS-GI specimen analysed by XRF

Oxide:	Net	Wt%	At%	I-Error%
Al_2O_3	30.77	17.5969	15.17	1.93
SiO_2	78.91	29.065	42.53	1.16
P_2O_5	49.08	13.1326	8.13	1.49
CaO	391.93	17.809	27.92	0.51
La_2O_3	270.81	21.7491	5.87	0.62
Cr_2O_3	18.44	0.5816	0.34	2.77
Fe_2O_3	2.96	0.0658	0.04	11.27

Weight percentage and atomic percentage of elemental compositions of 30%CS-GI specimen analysed by XRF

Oxide:	Net	Wt%	At%	I-Error%
Al_2O_3	24.61	14.5138	11.4	2.24
SiO_2	100.13	37.2866	49.7	1.03
P_2O_5	16.55	4.7184	2.66	2.88
CaO	452.52	21.1932	30.27	0.47
La_2O_3	245.47	21.1648	5.2	0.65
Cr_2O_3	19.66	0.664	0.35	2.71
MnO	9.79	0.2279	0.26	4.43
Fe_2O_3	2.96	0.0692	0.03	12.26
SrO	11.77	0.1621	0.13	5.81

Weight percentage and atomic percentage of elemental compositions of 28-day-soaked 30%CS-GI specimen analysed by XRF

Oxide:	Net	Wt%	At%	I-Error%
Al_2O_3	25.6	13.9811	11.41	2.2
SiO_2	108.65	37.5055	51.95	0.99
P_2O_5	43.52	11.6141	6.81	1.63
CaO	372.49	16.4781	24.45	0.52
La_2O_3	259.79	19.8473	5.07	0.63
Cr_2O_3	16.77	0.5013	0.27	2.95
Fe_2O_3	3.51	0.0725	0.04	9.9

Weight percentage and atomic percentage of elemental compositions of 50%CS-GI specimen analysed by XRF

Oxide:	Net	Wt%	At%	I-Error%
Al_2O_3	25.94	11.3979	7.99	2.17
SiO_2	178.95	49.5778	58.96	0.76
P_2O_5	19.57	4.6524	2.34	2.57
CaO	572.6	21.7603	27.73	0.42
La_2O_3	175.8	12.0733	2.65	0.77
Cr_2O_3	12.05	0.3179	0.15	3.77
MnO	7.09	0.1164	0.12	5.65
Fe_2O_3	2.41	0.0384	0.02	14.52
SrO	7.21	0.0656	0.05	9.03

Weight percentage and atomic percentage of elemental compositions of 28-day-soaked 50%CS-GI specimen analysed by XRF

Oxide:	Net	Wt%	At%	I-Error%
Al_2O_3	19.45	10.7777	8.09	2.54
SiO_2	133.02	45.9289	58.47	0.88
P_2O_5	32.91	9.4413	5.09	1.88
CaO	384.89	17.9653	24.5	0.51
La_2O_3	190.62	15.4328	3.62	0.73
Cr_2O_3	11.59	0.3637	0.18	3.63
Fe_2O_3	4.46	0.0903	0.04	7.75

Weight percentage and atomic percentage of elemental compositions of MTA specimen analysed by XRF

Oxide:	Net	Wt%	At%	I-Error%
Al_2O_3	4.66	1.5522	1.24	5.99
SiO_2	93.42	16.4317	22.32	1.05
P_2O_5	11.43	1.4094	0.81	3.31
CaO	1217.09	47.9584	69.81	0.29
Fe_2O_3	17.68	0.2672	0.14	2.9
Bi_2O_3	1177.2	32.3811	5.67	0.29

Weight percentage and atomic percentage of elemental compositions of 28-day-soaked MTA specimen analysed by XRF

Oxide:	Net	Wt%	At%	I-Error%
P2O5	387.88	36.1306	23.01	0.51
CaO	1455.75	45.5281	73.4	0.26
MnO	0.42	0.0052	0.01	65.72
Fe2O3	3.68	0.0438	0.02	9.68
Bi2O3	889.07	18.2924	3.55	0.34

Descriptive statistic analysis of percentage of cell viability from all groups

Descriptive Statistics

	N	Minimum	Maximum	Mean	Std. Deviation
data	360	26.4700	153.8900	96.280833	17.2540071
Valid N (listwise)	360				

One-way analysis of variance of percentage of cell viability from all groups

ANOVA

	Sum of Squares	df	Mean Square	F	Sig.
Between Groups	53373.457	19	2809.129	17.852	.000
Within Groups	53501.115	340	157.356		
Total	106874.573	359			

Post Hoc comparisons with Scheffé's test

Multiple Comparisons

(I) matconc	(J) matconc	Mean Difference (I-J)	Std. Error	Sig.	95% Confidence Interval	
					Lower Bound	Upper Bound
GI100%	GI1:1	-41.2611111*	4.1813903	.000	-64.439445	-18.082778
	GI1:2	-52.2727778*	4.1813903	.000	-75.451111	-29.094444
	GI1:4	-57.0583333*	4.1813903	.000	-80.236667	-33.880000
	10%CS-GIC 100%	-22.8094444	4.1813903	.062	-45.987778	.368889
	10%CS-GIC 1:1	-48.1383333*	4.1813903	.000	-71.316667	-24.960000
	10%CS-GIC 1:2	-53.0805556*	4.1813903	.000	-76.258889	-29.902222
	10%CS-GIC 1:4	-50.1250000*	4.1813903	.000	-73.303334	-26.946666
	30%CS-GIC 100%	-39.8250000*	4.1813903	.000	-63.003334	-16.646666
	30%CS-GIC 1:1	-44.5094444*	4.1813903	.000	-67.687778	-21.331111
	30%CS-GIC 1:2	-46.6333333*	4.1813903	.000	-69.811667	-23.455000
	30%CS-GIC 1:4	-49.8577778*	4.1813903	.000	-73.036111	-26.679444
	50%CS-GIC 100%	-48.1161111*	4.1813903	.000	-71.294445	-24.937778
	50%CS-GIC 1:1	-47.6633333*	4.1813903	.000	-70.841667	-24.485000
	50%CS-GIC 1:2	-50.9405556*	4.1813903	.000	-74.118889	-27.762222
	50%CS-GIC 1:4	-49.9472222*	4.1813903	.000	-73.125556	-26.768889
	MTA 100%	-41.5472222*	4.1813903	.000	-64.725556	-18.368889
	MTA 1:1	-40.2088889*	4.1813903	.000	-63.387222	-17.030555
	MTA 1:2	-42.5555556*	4.1813903	.000	-65.733889	-19.377222
	MTA 1:4	-46.0111111*	4.1813903	.000	-69.189445	-22.832778

GI1:1	GI100%	41.2611111*	4.1813903	.000	18.082778	64.439445
	GI1:2	-11.0116667	4.1813903	.994	-34.190000	12.166667
	GI1:4	-15.7972222	4.1813903	.764	-38.975556	7.381111
	10%CS-GIC 100%	18.4516667	4.1813903	.431	-4.726667	41.630000
	10%CS-GIC 1:1	-6.8772222	4.1813903	1.000	-30.055556	16.301111
	10%CS-GIC 1:2	-11.8194444	4.1813903	.986	-34.997778	11.358889
	10%CS-GIC 1:4	-8.8638889	4.1813903	1.000	-32.042222	14.314445
	30%CS-GIC 100%	1.4361111	4.1813903	1.000	-21.742222	24.614445
	30%CS-GIC 1:1	-3.2483333	4.1813903	1.000	-26.426667	19.930000
	30%CS-GIC 1:2	-5.3722222	4.1813903	1.000	-28.550556	17.806111
	30%CS-GIC 1:4	-8.5966667	4.1813903	1.000	-31.775000	14.581667
	50%CS-GIC 100%	-6.8550000	4.1813903	1.000	-30.033334	16.323334
	50%CS-GIC 1:1	-6.4022222	4.1813903	1.000	-29.580556	16.776111
	50%CS-GIC 1:2	-9.6794444	4.1813903	.999	-32.857778	13.498889
	50%CS-GIC 1:4	-8.6861111	4.1813903	1.000	-31.864445	14.492222
	MTA 100%	-.2861111	4.1813903	1.000	-23.464445	22.892222
	MTA 1:1	1.0522222	4.1813903	1.000	-22.126111	24.230556
	MTA 1:2	-1.2944444	4.1813903	1.000	-24.472778	21.883889
	MTA 1:4	-4.7500000	4.1813903	1.000	-27.928334	18.428334
GI1:2	GI100%	52.2727778*	4.1813903	.000	29.094444	75.451111
	GI1:1	11.0116667	4.1813903	.994	-12.166667	34.190000
	GI1:4	-4.7855556	4.1813903	1.000	-27.963889	18.392778
	10%CS-GIC 100%	29.4633333*	4.1813903	.000	6.285000	52.641667
	10%CS-GIC 1:1	4.1344444	4.1813903	1.000	-19.043889	27.312778
	10%CS-GIC 1:2	-.8077778	4.1813903	1.000	-23.986111	22.370556
	10%CS-GIC 1:4	2.1477778	4.1813903	1.000	-21.030556	25.326111
	30%CS-GIC 100%	12.4477778	4.1813903	.974	-10.730556	35.626111
	30%CS-GIC 1:1	7.7633333	4.1813903	1.000	-15.415000	30.941667
	30%CS-GIC 1:2	5.6394444	4.1813903	1.000	-17.538889	28.817778
	30%CS-GIC 1:4	2.4150000	4.1813903	1.000	-20.763334	25.593334
	50%CS-GIC 100%	4.1566667	4.1813903	1.000	-19.021667	27.335000
	50%CS-GIC 1:1	4.6094444	4.1813903	1.000	-18.568889	27.787778
	50%CS-GIC 1:2	1.3322222	4.1813903	1.000	-21.846111	24.510556
	50%CS-GIC 1:4	2.3255556	4.1813903	1.000	-20.852778	25.503889

	MTA 100%	10.7255556	4.1813903	.996	-12.452778	33.903889
	MTA 1:1	12.0638889	4.1813903	.982	-11.114445	35.242222
	MTA 1:2	9.7172222	4.1813903	.999	-13.461111	32.895556
	MTA 1:4	6.2616667	4.1813903	1.000	-16.916667	29.440000
GI1:4	GI100%	57.0583333*	4.1813903	.000	33.880000	80.236667
	GI1:1	15.7972222	4.1813903	.764	-7.381111	38.975556
	GI1:2	4.7855556	4.1813903	1.000	-18.392778	27.963889
	10%CS-GIC 100%	34.2488889*	4.1813903	.000	11.070555	57.427222
	10%CS-GIC 1:1	8.9200000	4.1813903	1.000	-14.258334	32.098334
	10%CS-GIC 1:2	3.9777778	4.1813903	1.000	-19.200556	27.156111
	10%CS-GIC 1:4	6.9333333	4.1813903	1.000	-16.245000	30.111667
	30%CS-GIC 100%	17.2333333	4.1813903	.591	-5.945000	40.411667
	30%CS-GIC 1:1	12.5488889	4.1813903	.972	-10.629445	35.727222
	30%CS-GIC 1:2	10.4250000	4.1813903	.997	-12.753334	33.603334
	30%CS-GIC 1:4	7.2005556	4.1813903	1.000	-15.977778	30.378889
	50%CS-GIC 100%	8.9422222	4.1813903	1.000	-14.236111	32.120556
	50%CS-GIC 1:1	9.3950000	4.1813903	.999	-13.783334	32.573334
	50%CS-GIC 1:2	6.1177778	4.1813903	1.000	-17.060556	29.296111
	50%CS-GIC 1:4	7.1111111	4.1813903	1.000	-16.067222	30.289445
	MTA 100%	15.5111111	4.1813903	.794	-7.667222	38.689445
	MTA 1:1	16.8494444	4.1813903	.640	-6.328889	40.027778
	MTA 1:2	14.5027778	4.1813903	.881	-8.675556	37.681111
	MTA 1:4	11.0472222	4.1813903	.994	-12.131111	34.225556
10%CS-GIC 100%	GI100%	22.8094444	4.1813903	.062	-.368889	45.987778
	GI1:1	-18.4516667	4.1813903	.431	-41.630000	4.726667
	GI1:2	-29.4633333*	4.1813903	.000	-52.641667	-6.285000
	GI1:4	-34.2488889*	4.1813903	.000	-57.427222	-11.070555
	10%CS-GIC 1:1	-25.3288889*	4.1813903	.011	-48.507222	-2.150555
	10%CS-GIC 1:2	-30.2711111*	4.1813903	.000	-53.449445	-7.092778
	10%CS-GIC 1:4	-27.3155556*	4.1813903	.002	-50.493889	-4.137222
	30%CS-GIC 100%	-17.0155556	4.1813903	.619	-40.193889	6.162778
	30%CS-GIC 1:1	-21.7000000	4.1813903	.115	-44.878334	1.478334
	30%CS-GIC 1:2	-23.8238889*	4.1813903	.033	-47.002222	-.645555
	30%CS-GIC 1:4	-27.0483333*	4.1813903	.003	-50.226667	-3.870000

	50%CS-GIC 100%	-25.3066667*	4.1813903	.012	-48.485000	-2.128333
	50%CS-GIC 1:1	-24.8538889*	4.1813903	.016	-48.032222	-1.675555
	50%CS-GIC 1:2	-28.1311111*	4.1813903	.001	-51.309445	-4.952778
	50%CS-GIC 1:4	-27.1377778*	4.1813903	.003	-50.316111	-3.959444
	MTA 100%	-18.7377778	4.1813903	.395	-41.916111	4.440556
	MTA 1:1	-17.3994444	4.1813903	.569	-40.577778	5.778889
	MTA 1:2	-19.7461111	4.1813903	.278	-42.924445	3.432222
	MTA 1:4	-23.2016667*	4.1813903	.049	-46.380000	-.023333
10%CS-GIC 1:1	GI100%	48.1383333*	4.1813903	.000	24.960000	71.316667
	GI1:1	6.8772222	4.1813903	1.000	-16.301111	30.055556
	GI1:2	-4.1344444	4.1813903	1.000	-27.312778	19.043889
	GI1:4	-8.9200000	4.1813903	1.000	-32.098334	14.258334
	10%CS-GIC 100%	25.3288889*	4.1813903	.011	2.150555	48.507222
	10%CS-GIC 1:2	-4.9422222	4.1813903	1.000	-28.120556	18.236111
	10%CS-GIC 1:4	-1.9866667	4.1813903	1.000	-25.165000	21.191667
	30%CS-GIC 100%	8.3133333	4.1813903	1.000	-14.865000	31.491667
	30%CS-GIC 1:1	3.6288889	4.1813903	1.000	-19.549445	26.807222
	30%CS-GIC 1:2	1.5050000	4.1813903	1.000	-21.673334	24.683334
	30%CS-GIC 1:4	-1.7194444	4.1813903	1.000	-24.897778	21.458889
	50%CS-GIC 100%	.0222222	4.1813903	1.000	-23.156111	23.200556
	50%CS-GIC 1:1	.4750000	4.1813903	1.000	-22.703334	23.653334
	50%CS-GIC 1:2	-2.8022222	4.1813903	1.000	-25.980556	20.376111
	50%CS-GIC 1:4	-1.8088889	4.1813903	1.000	-24.987222	21.369445
	MTA 100%	6.5911111	4.1813903	1.000	-16.587222	29.769445
	MTA 1:1	7.9294444	4.1813903	1.000	-15.248889	31.107778
	MTA 1:2	5.5827778	4.1813903	1.000	-17.595556	28.761111
	MTA 1:4	2.1272222	4.1813903	1.000	-21.051111	25.305556
10%CS-GIC 1:2	GI100%	53.0805556*	4.1813903	.000	29.902222	76.258889
	GI1:1	11.8194444	4.1813903	.986	-11.358889	34.997778
	GI1:2	.8077778	4.1813903	1.000	-22.370556	23.986111
	GI1:4	-3.9777778	4.1813903	1.000	-27.156111	19.200556
	10%CS-GIC 100%	30.2711111*	4.1813903	.000	7.092778	53.449445
	10%CS-GIC 1:1	4.9422222	4.1813903	1.000	-18.236111	28.120556
	10%CS-GIC 1:4	2.9555556	4.1813903	1.000	-20.222778	26.133889

	30%CS-GIC 100%	13.2555556	4.1813903	.949	-9.922778	36.433889
	30%CS-GIC 1:1	8.5711111	4.1813903	1.000	-14.607222	31.749445
	30%CS-GIC 1:2	6.4472222	4.1813903	1.000	-16.731111	29.625556
	30%CS-GIC 1:4	3.2227778	4.1813903	1.000	-19.955556	26.401111
	50%CS-GIC 100%	4.9644444	4.1813903	1.000	-18.213889	28.142778
	50%CS-GIC 1:1	5.4172222	4.1813903	1.000	-17.761111	28.595556
	50%CS-GIC 1:2	2.1400000	4.1813903	1.000	-21.038334	25.318334
	50%CS-GIC 1:4	3.1333333	4.1813903	1.000	-20.045000	26.311667
	MTA 100%	11.5333333	4.1813903	.989	-11.645000	34.711667
	MTA 1:1	12.8716667	4.1813903	.963	-10.306667	36.050000
	MTA 1:2	10.5250000	4.1813903	.997	-12.653334	33.703334
	MTA 1:4	7.0694444	4.1813903	1.000	-16.108889	30.247778
10%CS-GIC 1:4	GI100%	50.1250000*	4.1813903	.000	26.946666	73.303334
	GI1:1	8.8638889	4.1813903	1.000	-14.314445	32.042222
	GI1:2	-2.1477778	4.1813903	1.000	-25.326111	21.030556
	GI1:4	-6.9333333	4.1813903	1.000	-30.111667	16.245000
	10%CS-GIC 100%	27.3155556*	4.1813903	.002	4.137222	50.493889
	10%CS-GIC 1:1	1.9866667	4.1813903	1.000	-21.191667	25.165000
	10%CS-GIC 1:2	-2.9555556	4.1813903	1.000	-26.133889	20.222778
	30%CS-GIC 100%	10.3000000	4.1813903	.998	-12.878334	33.478334
	30%CS-GIC 1:1	5.6155556	4.1813903	1.000	-17.562778	28.793889
	30%CS-GIC 1:2	3.4916667	4.1813903	1.000	-19.686667	26.670000
	30%CS-GIC 1:4	.2672222	4.1813903	1.000	-22.911111	23.445556
	50%CS-GIC 100%	2.0088889	4.1813903	1.000	-21.169445	25.187222
	50%CS-GIC 1:1	2.4616667	4.1813903	1.000	-20.716667	25.640000
	50%CS-GIC 1:2	-.8155556	4.1813903	1.000	-23.993889	22.362778
	50%CS-GIC 1:4	.1777778	4.1813903	1.000	-23.000556	23.356111
	MTA 100%	8.5777778	4.1813903	1.000	-14.600556	31.756111
	MTA 1:1	9.9161111	4.1813903	.999	-13.262222	33.094445
	MTA 1:2	7.5694444	4.1813903	1.000	-15.608889	30.747778
	MTA 1:4	4.1138889	4.1813903	1.000	-19.064445	27.292222
30%CS-GIC 100%	GI100%	39.8250000*	4.1813903	.000	16.646666	63.003334
	GI1:1	-1.4361111	4.1813903	1.000	-24.614445	21.742222
	GI1:2	-12.4477778	4.1813903	.974	-35.626111	10.730556

	GI1:4	-17.2333333	4.1813903	.591	-40.411667	5.945000
	10%CS-GIC 100%	17.0155556	4.1813903	.619	-6.162778	40.193889
	10%CS-GIC 1:1	-8.3133333	4.1813903	1.000	-31.491667	14.865000
	10%CS-GIC 1:2	-13.2555556	4.1813903	.949	-36.433889	9.922778
	10%CS-GIC 1:4	-10.3000000	4.1813903	.998	-33.478334	12.878334
	30%CS-GIC 1:1	-4.6844444	4.1813903	1.000	-27.862778	18.493889
	30%CS-GIC 1:2	-6.8083333	4.1813903	1.000	-29.986667	16.370000
	30%CS-GIC 1:4	-10.0327778	4.1813903	.998	-33.211111	13.145556
	50%CS-GIC 100%	-8.2911111	4.1813903	1.000	-31.469445	14.887222
	50%CS-GIC 1:1	-7.8383333	4.1813903	1.000	-31.016667	15.340000
	50%CS-GIC 1:2	-11.1155556	4.1813903	.993	-34.293889	12.062778
	50%CS-GIC 1:4	-10.1222222	4.1813903	.998	-33.300556	13.056111
	MTA 100%	-1.7222222	4.1813903	1.000	-24.900556	21.456111
	MTA 1:1	-.3838889	4.1813903	1.000	-23.562222	22.794445
	MTA 1:2	-2.7305556	4.1813903	1.000	-25.908889	20.447778
	MTA 1:4	-6.1861111	4.1813903	1.000	-29.364445	16.992222
30%CS-GIC 1:1	GI100%	44.5094444*	4.1813903	.000	21.331111	67.687778
	GI1:1	3.2483333	4.1813903	1.000	-19.930000	26.426667
	GI1:2	-7.7633333	4.1813903	1.000	-30.941667	15.415000
	GI1:4	-12.5488889	4.1813903	.972	-35.727222	10.629445
	10%CS-GIC 100%	21.7000000	4.1813903	.115	-1.478334	44.878334
	10%CS-GIC 1:1	-3.6288889	4.1813903	1.000	-26.807222	19.549445
	10%CS-GIC 1:2	-8.5711111	4.1813903	1.000	-31.749445	14.607222
	10%CS-GIC 1:4	-5.6155556	4.1813903	1.000	-28.793889	17.562778
	30%CS-GIC 100%	4.6844444	4.1813903	1.000	-18.493889	27.862778
	30%CS-GIC 1:2	-2.1238889	4.1813903	1.000	-25.302222	21.054445
	30%CS-GIC 1:4	-5.3483333	4.1813903	1.000	-28.526667	17.830000
	50%CS-GIC 100%	-3.6066667	4.1813903	1.000	-26.785000	19.571667
	50%CS-GIC 1:1	-3.1538889	4.1813903	1.000	-26.332222	20.024445
	50%CS-GIC 1:2	-6.4311111	4.1813903	1.000	-29.609445	16.747222
	50%CS-GIC 1:4	-5.4377778	4.1813903	1.000	-28.616111	17.740556
	MTA 100%	2.9622222	4.1813903	1.000	-20.216111	26.140556
	MTA 1:1	4.3005556	4.1813903	1.000	-18.877778	27.478889
	MTA 1:2	1.9538889	4.1813903	1.000	-21.224445	25.132222

	MTA 1:4	-1.5016667	4.1813903	1.000	-24.680000	21.676667
30%CS-GIC 1:2	GI100%	46.6333333*	4.1813903	.000	23.455000	69.811667
	GI1:1	5.3722222	4.1813903	1.000	-17.806111	28.550556
	GI1:2	-5.6394444	4.1813903	1.000	-28.817778	17.538889
	GI1:4	-10.4250000	4.1813903	.997	-33.603334	12.753334
	10%CS-GIC 100%	23.8238889*	4.1813903	.033	.645555	47.002222
	10%CS-GIC 1:1	-1.5050000	4.1813903	1.000	-24.683334	21.673334
	10%CS-GIC 1:2	-6.4472222	4.1813903	1.000	-29.625556	16.731111
	10%CS-GIC 1:4	-3.4916667	4.1813903	1.000	-26.670000	19.686667
	30%CS-GIC 100%	6.8083333	4.1813903	1.000	-16.370000	29.986667
	30%CS-GIC 1:1	2.1238889	4.1813903	1.000	-21.054445	25.302222
	30%CS-GIC 1:4	-3.2244444	4.1813903	1.000	-26.402778	19.953889
	50%CS-GIC 100%	-1.4827778	4.1813903	1.000	-24.661111	21.695556
	50%CS-GIC 1:1	-1.0300000	4.1813903	1.000	-24.208334	22.148334
	50%CS-GIC 1:2	-4.3072222	4.1813903	1.000	-27.485556	18.871111
	50%CS-GIC 1:4	-3.3138889	4.1813903	1.000	-26.492222	19.864445
	MTA 100%	5.0861111	4.1813903	1.000	-18.092222	28.264445
	MTA 1:1	6.4244444	4.1813903	1.000	-16.753889	29.602778
	MTA 1:2	4.0777778	4.1813903	1.000	-19.100556	27.256111
	MTA 1:4	.6222222	4.1813903	1.000	-22.556111	23.800556
30%CS-GIC 1:4	GI100%	49.8577778*	4.1813903	.000	26.679444	73.036111
	GI1:1	8.5966667	4.1813903	1.000	-14.581667	31.775000
	GI1:2	-2.4150000	4.1813903	1.000	-25.593334	20.763334
	GI1:4	-7.2005556	4.1813903	1.000	-30.378889	15.977778
	10%CS-GIC 100%	27.0483333*	4.1813903	.003	3.870000	50.226667
	10%CS-GIC 1:1	1.7194444	4.1813903	1.000	-21.458889	24.897778
	10%CS-GIC 1:2	-3.2227778	4.1813903	1.000	-26.401111	19.955556
	10%CS-GIC 1:4	-.2672222	4.1813903	1.000	-23.445556	22.911111
	30%CS-GIC 100%	10.0327778	4.1813903	.998	-13.145556	33.211111
	30%CS-GIC 1:1	5.3483333	4.1813903	1.000	-17.830000	28.526667
	30%CS-GIC 1:2	3.2244444	4.1813903	1.000	-19.953889	26.402778
	50%CS-GIC 100%	1.7416667	4.1813903	1.000	-21.436667	24.920000
	50%CS-GIC 1:1	2.1944444	4.1813903	1.000	-20.983889	25.372778
	50%CS-GIC 1:2	-1.0827778	4.1813903	1.000	-24.261111	22.095556

	50%CS-GIC 1:4	-.0894444	4.1813903	1.000	-23.267778	23.088889
	MTA 100%	8.3105556	4.1813903	1.000	-14.867778	31.488889
	MTA 1:1	9.6488889	4.1813903	.999	-13.529445	32.827222
	MTA 1:2	7.3022222	4.1813903	1.000	-15.876111	30.480556
	MTA 1:4	3.8466667	4.1813903	1.000	-19.331667	27.025000
50%CS-GIC 100%	GI100%	48.1161111*	4.1813903	.000	24.937778	71.294445
	GI1:1	6.8550000	4.1813903	1.000	-16.323334	30.033334
	GI1:2	-4.1566667	4.1813903	1.000	-27.335000	19.021667
	GI1:4	-8.9422222	4.1813903	1.000	-32.120556	14.236111
	10%CS-GIC 100%	25.3066667*	4.1813903	.012	2.128333	48.485000
	10%CS-GIC 1:1	-.0222222	4.1813903	1.000	-23.200556	23.156111
	10%CS-GIC 1:2	-4.9644444	4.1813903	1.000	-28.142778	18.213889
	10%CS-GIC 1:4	-2.0088889	4.1813903	1.000	-25.187222	21.169445
	30%CS-GIC 100%	8.2911111	4.1813903	1.000	-14.887222	31.469445
	30%CS-GIC 1:1	3.6066667	4.1813903	1.000	-19.571667	26.785000
	30%CS-GIC 1:2	1.4827778	4.1813903	1.000	-21.695556	24.661111
	30%CS-GIC 1:4	-1.7416667	4.1813903	1.000	-24.920000	21.436667
	50%CS-GIC 1:1	.4527778	4.1813903	1.000	-22.725556	23.631111
	50%CS-GIC 1:2	-2.8244444	4.1813903	1.000	-26.002778	20.353889
	50%CS-GIC 1:4	-1.8311111	4.1813903	1.000	-25.009445	21.347222
	MTA 100%	6.5688889	4.1813903	1.000	-16.609445	29.747222
	MTA 1:1	7.9072222	4.1813903	1.000	-15.271111	31.085556
	MTA 1:2	5.5605556	4.1813903	1.000	-17.617778	28.738889
	MTA 1:4	2.1050000	4.1813903	1.000	-21.073334	25.283334
50%CS-GIC 1:1	GI100%	47.6633333*	4.1813903	.000	24.485000	70.841667
	GI1:1	6.4022222	4.1813903	1.000	-16.776111	29.580556
	GI1:2	-4.6094444	4.1813903	1.000	-27.787778	18.568889
	GI1:4	-9.3950000	4.1813903	.999	-32.573334	13.783334
	10%CS-GIC 100%	24.8538889*	4.1813903	.016	1.675555	48.032222
	10%CS-GIC 1:1	-.4750000	4.1813903	1.000	-23.653334	22.703334
	10%CS-GIC 1:2	-5.4172222	4.1813903	1.000	-28.595556	17.761111
	10%CS-GIC 1:4	-2.4616667	4.1813903	1.000	-25.640000	20.716667
	30%CS-GIC 100%	7.8383333	4.1813903	1.000	-15.340000	31.016667
	30%CS-GIC 1:1	3.1538889	4.1813903	1.000	-20.024445	26.332222

	30%CS-GIC 1:2	1.0300000	4.1813903	1.000	-22.148334	24.208334
	30%CS-GIC 1:4	-2.1944444	4.1813903	1.000	-25.372778	20.983889
	50%CS-GIC 100%	-.4527778	4.1813903	1.000	-23.631111	22.725556
	50%CS-GIC 1:2	-3.2772222	4.1813903	1.000	-26.455556	19.901111
	50%CS-GIC 1:4	-2.2838889	4.1813903	1.000	-25.462222	20.894445
	MTA 100%	6.1161111	4.1813903	1.000	-17.062222	29.294445
	MTA 1:1	7.4544444	4.1813903	1.000	-15.723889	30.632778
	MTA 1:2	5.1077778	4.1813903	1.000	-18.070556	28.286111
	MTA 1:4	1.6522222	4.1813903	1.000	-21.526111	24.830556
50%CS-GIC 1:2	GI100%	50.9405556*	4.1813903	.000	27.762222	74.118889
	GI1:1	9.6794444	4.1813903	.999	-13.498889	32.857778
	GI1:2	-1.3322222	4.1813903	1.000	-24.510556	21.846111
	GI1:4	-6.1177778	4.1813903	1.000	-29.296111	17.060556
	10%CS-GIC 100%	28.1311111*	4.1813903	.001	4.952778	51.309445
	10%CS-GIC 1:1	2.8022222	4.1813903	1.000	-20.376111	25.980556
	10%CS-GIC 1:2	-2.1400000	4.1813903	1.000	-25.318334	21.038334
	10%CS-GIC 1:4	.8155556	4.1813903	1.000	-22.362778	23.993889
	30%CS-GIC 100%	11.1155556	4.1813903	.993	-12.062778	34.293889
	30%CS-GIC 1:1	6.4311111	4.1813903	1.000	-16.747222	29.609445
	30%CS-GIC 1:2	4.3072222	4.1813903	1.000	-18.871111	27.485556
	30%CS-GIC 1:4	1.0827778	4.1813903	1.000	-22.095556	24.261111
	50%CS-GIC 100%	2.8244444	4.1813903	1.000	-20.353889	26.002778
	50%CS-GIC 1:1	3.2772222	4.1813903	1.000	-19.901111	26.455556
	50%CS-GIC 1:4	.9933333	4.1813903	1.000	-22.185000	24.171667
	MTA 100%	9.3933333	4.1813903	.999	-13.785000	32.571667
	MTA 1:1	10.7316667	4.1813903	.996	-12.446667	33.910000
	MTA 1:2	8.3850000	4.1813903	1.000	-14.793334	31.563334
	MTA 1:4	4.9294444	4.1813903	1.000	-18.248889	28.107778
50%CS-GIC 1:4	GI100%	49.9472222*	4.1813903	.000	26.768889	73.125556
	GI1:1	8.6861111	4.1813903	1.000	-14.492222	31.864445
	GI1:2	-2.3255556	4.1813903	1.000	-25.503889	20.852778
	GI1:4	-7.1111111	4.1813903	1.000	-30.289445	16.067222
	10%CS-GIC 100%	27.1377778*	4.1813903	.003	3.959444	50.316111
	10%CS-GIC 1:1	1.8088889	4.1813903	1.000	-21.369445	24.987222

	10%CS-GIC 1:2	-3.1333333	4.1813903	1.000	-26.311667	20.045000
	10%CS-GIC 1:4	-.1777778	4.1813903	1.000	-23.356111	23.000556
	30%CS-GIC 100%	10.1222222	4.1813903	.998	-13.056111	33.300556
	30%CS-GIC 1:1	5.4377778	4.1813903	1.000	-17.740556	28.616111
	30%CS-GIC 1:2	3.3138889	4.1813903	1.000	-19.864445	26.492222
	30%CS-GIC 1:4	.0894444	4.1813903	1.000	-23.088889	23.267778
	50%CS-GIC 100%	1.8311111	4.1813903	1.000	-21.347222	25.009445
	50%CS-GIC 1:1	2.2838889	4.1813903	1.000	-20.894445	25.462222
	50%CS-GIC 1:2	-.9933333	4.1813903	1.000	-24.171667	22.185000
	MTA 100%	8.4000000	4.1813903	1.000	-14.778334	31.578334
	MTA 1:1	9.7383333	4.1813903	.999	-13.440000	32.916667
	MTA 1:2	7.3916667	4.1813903	1.000	-15.786667	30.570000
	MTA 1:4	3.9361111	4.1813903	1.000	-19.242222	27.114445
MTA 100%	GI100%	41.5472222*	4.1813903	.000	18.368889	64.725556
	GI1:1	.2861111	4.1813903	1.000	-22.892222	23.464445
	GI1:2	-10.7255556	4.1813903	.996	-33.903889	12.452778
	GI1:4	-15.5111111	4.1813903	.794	-38.689445	7.667222
	10%CS-GIC 100%	18.7377778	4.1813903	.395	-4.440556	41.916111
	10%CS-GIC 1:1	-6.5911111	4.1813903	1.000	-29.769445	16.587222
	10%CS-GIC 1:2	-11.5333333	4.1813903	.989	-34.711667	11.645000
	10%CS-GIC 1:4	-8.5777778	4.1813903	1.000	-31.756111	14.600556
	30%CS-GIC 100%	1.7222222	4.1813903	1.000	-21.456111	24.900556
	30%CS-GIC 1:1	-2.9622222	4.1813903	1.000	-26.140556	20.216111
	30%CS-GIC 1:2	-5.0861111	4.1813903	1.000	-28.264445	18.092222
	30%CS-GIC 1:4	-8.3105556	4.1813903	1.000	-31.488889	14.867778
	50%CS-GIC 100%	-6.5688889	4.1813903	1.000	-29.747222	16.609445
	50%CS-GIC 1:1	-6.1161111	4.1813903	1.000	-29.294445	17.062222
	50%CS-GIC 1:2	-9.3933333	4.1813903	.999	-32.571667	13.785000
	50%CS-GIC 1:4	-8.4000000	4.1813903	1.000	-31.578334	14.778334
	MTA 1:1	1.3383333	4.1813903	1.000	-21.840000	24.516667
	MTA 1:2	-1.0083333	4.1813903	1.000	-24.186667	22.170000
	MTA 1:4	-4.4638889	4.1813903	1.000	-27.642222	18.714445
MTA 1:1	GI100%	40.2088889*	4.1813903	.000	17.030555	63.387222
	GI1:1	-1.0522222	4.1813903	1.000	-24.230556	22.126111

	GI1:2	-12.0638889	4.1813903	.982	-35.242222	11.114445
	GI1:4	-16.8494444	4.1813903	.640	-40.027778	6.328889
	10%CS-GIC 100%	17.3994444	4.1813903	.569	-5.778889	40.577778
	10%CS-GIC 1:1	-7.9294444	4.1813903	1.000	-31.107778	15.248889
	10%CS-GIC 1:2	-12.8716667	4.1813903	.963	-36.050000	10.306667
	10%CS-GIC 1:4	-9.9161111	4.1813903	.999	-33.094445	13.262222
	30%CS-GIC 100%	.3838889	4.1813903	1.000	-22.794445	23.562222
	30%CS-GIC 1:1	-4.3005556	4.1813903	1.000	-27.478889	18.877778
	30%CS-GIC 1:2	-6.4244444	4.1813903	1.000	-29.602778	16.753889
	30%CS-GIC 1:4	-9.6488889	4.1813903	.999	-32.827222	13.529445
	50%CS-GIC 100%	-7.9072222	4.1813903	1.000	-31.085556	15.271111
	50%CS-GIC 1:1	-7.4544444	4.1813903	1.000	-30.632778	15.723889
	50%CS-GIC 1:2	-10.7316667	4.1813903	.996	-33.910000	12.446667
	50%CS-GIC 1:4	-9.7383333	4.1813903	.999	-32.916667	13.440000
	MTA 100%	-1.3383333	4.1813903	1.000	-24.516667	21.840000
	MTA 1:2	-2.3466667	4.1813903	1.000	-25.525000	20.831667
	MTA 1:4	-5.8022222	4.1813903	1.000	-28.980556	17.376111
MTA 1:2	GI100%	42.5555556*	4.1813903	.000	19.377222	65.733889
	GI1:1	1.2944444	4.1813903	1.000	-21.883889	24.472778
	GI1:2	-9.7172222	4.1813903	.999	-32.895556	13.461111
	GI1:4	-14.5027778	4.1813903	.881	-37.681111	8.675556
	10%CS-GIC 100%	19.7461111	4.1813903	.278	-3.432222	42.924445
	10%CS-GIC 1:1	-5.5827778	4.1813903	1.000	-28.761111	17.595556
	10%CS-GIC 1:2	-10.5250000	4.1813903	.997	-33.703334	12.653334
	10%CS-GIC 1:4	-7.5694444	4.1813903	1.000	-30.747778	15.608889
	30%CS-GIC 100%	2.7305556	4.1813903	1.000	-20.447778	25.908889
	30%CS-GIC 1:1	-1.9538889	4.1813903	1.000	-25.132222	21.224445
	30%CS-GIC 1:2	-4.0777778	4.1813903	1.000	-27.256111	19.100556
	30%CS-GIC 1:4	-7.3022222	4.1813903	1.000	-30.480556	15.876111
	50%CS-GIC 100%	-5.5605556	4.1813903	1.000	-28.738889	17.617778
	50%CS-GIC 1:1	-5.1077778	4.1813903	1.000	-28.286111	18.070556
	50%CS-GIC 1:2	-8.3850000	4.1813903	1.000	-31.563334	14.793334
	50%CS-GIC 1:4	-7.3916667	4.1813903	1.000	-30.570000	15.786667
	MTA 100%	1.0083333	4.1813903	1.000	-22.170000	24.186667

	MTA 1:1	2.3466667	4.1813903	1.000	-20.831667	25.525000
	MTA 1:4	-3.4555556	4.1813903	1.000	-26.633889	19.722778
MTA 1:4	GI100%	46.0111111*	4.1813903	.000	22.832778	69.189445
	GI1:1	4.7500000	4.1813903	1.000	-18.428334	27.928334
	GI1:2	-6.2616667	4.1813903	1.000	-29.440000	16.916667
	GI1:4	-11.0472222	4.1813903	.994	-34.225556	12.131111
	10%CS-GIC 100%	23.2016667*	4.1813903	.049	.023333	46.380000
	10%CS-GIC 1:1	-2.1272222	4.1813903	1.000	-25.305556	21.051111
	10%CS-GIC 1:2	-7.0694444	4.1813903	1.000	-30.247778	16.108889
	10%CS-GIC 1:4	-4.1138889	4.1813903	1.000	-27.292222	19.064445
	30%CS-GIC 100%	6.1861111	4.1813903	1.000	-16.992222	29.364445
	30%CS-GIC 1:1	1.5016667	4.1813903	1.000	-21.676667	24.680000
	30%CS-GIC 1:2	-.6222222	4.1813903	1.000	-23.800556	22.556111
	30%CS-GIC 1:4	-3.8466667	4.1813903	1.000	-27.025000	19.331667
	50%CS-GIC 100%	-2.1050000	4.1813903	1.000	-25.283334	21.073334
	50%CS-GIC 1:1	-1.6522222	4.1813903	1.000	-24.830556	21.526111
	50%CS-GIC 1:2	-4.9294444	4.1813903	1.000	-28.107778	18.248889
	50%CS-GIC 1:4	-3.9361111	4.1813903	1.000	-27.114445	19.242222
	MTA 100%	4.4638889	4.1813903	1.000	-18.714445	27.642222
	MTA 1:1	5.8022222	4.1813903	1.000	-17.376111	28.980556
	MTA 1:2	3.4555556	4.1813903	1.000	-19.722778	26.633889

*. The mean difference is significant at the 0.05 level.

VITAE

VITAE

Name:	Mr. Wiroj Sangsawatpong
Date of birth:	25 February 1984
Place of birth:	Bangkok, Thailand
Address:	Chonburi, Thailand

Educational Background:

2002-2008	Doctor of Dental Surgery Srinakharinwirot University
2010-2013	Master of Science (Endodontology) Srinakharinwirot University